Department of Engineering Design and Production

Fault Simulator and Detection for a Process Control Valve

Timo Manninen

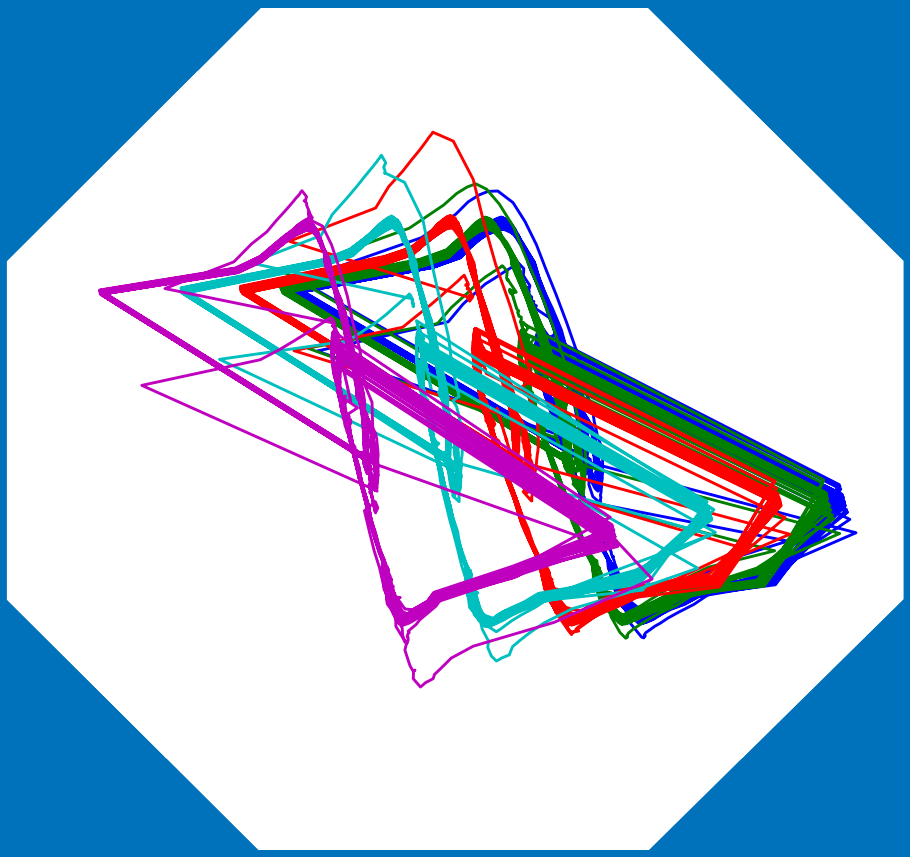

Aalto University

DOCTORAL DISSERTATIONS

Timo Manninen Fault Simulator and Detection for a Process Control Valve Aalto University

Aalto University publication series
DOCTORAL DISSERTATIONS 146/2012

Fault Simulator and Detection for a Process Control Valve

Timo Manninen

Doctoral dissertation for the degree of Doctor of Science in Technology to be presented with due permission of the School of Engineering for public examination and debate in Auditorium E at the Aalto University School of Engineering (Espoo, Finland) on the 30th of November 2012 at 12 noon.

Aalto University
School of Engineering
Department of Engineering Design and Production

Supervising professor
Prof. Matti Pietola

Thesis advisor
Jouni Pyötsiä (D.Sc.)

Preliminary examiners
Prof. Jouni Mattila, Tampere University of Technology, Finland
Prof. Eric Bideaux, INSA-Lyon, France

Opponents
Prof. Jouni Mattila, Tampere University of Technology, Finland
Prof. Kari Koskinen, Tampere University of Technology, Finland

Aalto University publication series
DOCTORAL DISSERTATIONS 146/2012

ISBN 978-952-60-4853-6 (printed)
ISBN 978-952-60-4854-3 (pdf)
ISSN-L 1799-4934
ISSN 1799-4934 (printed)
ISSN 1799-4942 (pdf)
http://urn.fi/URN:ISBN:978-952-60-4854-3

Unigrafia Oy
Helsinki 2012

Finland

441 697
Printed matter

Aalto University

Abstract

Aalto University, P.O. Box 11000, FI-00076 Aalto www.aalto.fi

Author
Timo Manninen

Name of the doctoral dissertation
Fault Simulator and Detection for a Process Control Valve

Publisher School of Engineering

Unit Department of Engineering Design and Production

Series Aalto University publication series DOCTORAL DISSERTATIONS 146/2012

Field of research Machine technology

Manuscript submitted 12 June 2012 **Date of the defence** 30 November 2012

Permission to publish granted (date) 15 October 2012 **Language** English

☒ **Monograph** ☐ **Article dissertation (summary + original articles)**

Abstract

In this study a novel fault simulator for a quarter-turn pneumatic control valve is presented. Another contribution of this study is a novel fault detection and diagnosis method for a control valve.

It has been possible to analytically model control valve dynamics, despite their inherent nonlinearities for the fault simulator. These nonlinearities of the system have been identified and estimated through selected parameters. The models that were derived have been verified with measurements and the modeling error is found to be acceptable for the fault simulations. Some typical control valve faults have been simulated and the impacts on the internal variables of the flow control loop and control performance analysed. The fault simulator presented here can be used for fault detection and diagnosis, as well as robust control research.

On the basis of simulations and test bench test runs it is possible to detect and diagnose typical control valve faults before they have a severe impact on flow control loop performance. This can be done with the online method introduced in this study, which requires low computing power. This means that the method is implementable in an intelligent valve controller and diagnosis can be performed without disturbing the process.

The method that is introduced is based on the observation that the internal variable closest to the fault compensates and reacts first to the fault when feedback control is utilised. That leads to an operation point shift for all the internal variables before the fault in the chain of the internal variables in the system. When these operation point changes are being detected, the faults can be detected and diagnosed. This principle can be utilised in all feedback-controlled mechatronic systems. The fault detection and diagnosis method introduced here was verified with the fault simulator and test bench runs and found to be applicable to the detection and diagnosis of all the faults that were tested.

Keywords fault simulator, fault detection, fault isolation, fault diagnosis, process control valve

ISBN (printed) 978-952-60-4853-6 **ISBN (pdf)** 978-952-60-4854-3

ISSN-L 1799-4934 **ISSN (printed)** 1799-4934 **ISSN (pdf)** 1799-4942

Location of publisher Espoo **Location of printing** Espoo **Year** 2012

Pages 75 **urn** http://urn.fi/URN:ISBN:978-952-60-4854-3

Tekijä
Timo Manninen

Väitöskirjan nimi
Vikasimulaattori ja vikojen havaitseminen prosessin säätöventtiilistä

Julkaisija Insinööritieteiden korkeakoulu

Yksikkö Koneenrakennustekniikan laitos

Sarja Aalto University publication series DOCTORAL DISSERTATIONS 146/2012

Tutkimusala Konetekniikka

Käsikirjoituksen pvm 12.06.2012 **Väitöspäivä** 30.11.2012

Julkaisuluvan myöntämispäivä 15.10.2012 **Kieli** Englanti

☒ **Monografia** ☐ **Yhdistelmäväitöskirja (yhteenveto-osa + erillisartikkelit)**

Tiivistelmä

Tässä työssä esitellään vikasimulaattori ja vikojen diagnosointimenetelmä pneumaattiselle prosessin säätöventtiilille.

Vikasimulaattoria varten säätöventtiili on mallinnettu ja sen epälineaarisuudet on identifioitu estimoitujen parametrien avulla. Lisäksi mallit on verifioitu laboratoriomittausten avulla ja mallinnusvirheen on todettu olevan riittävän pieni vikasimulaatioiden suorittamiseen. Joitakin säätöventtiilivikoja on simuloitu simulaattorissa ja niiden vaikutusta on analysoitu virtauksen säätöpiiriin sisäisiin muuttujiin ja säätöpiirin suorituskykyyn. Esiteltyä vikasimulaattoria voidaan käyttää, niin vikadiagnoosimenetelmien, kuin robustin säädönkin tutkimukseen.

Vikasimulaattorissa tehtyjen simulointien perusteella on mahdollista diagnosoida kaikki simuloidut viat ennenkuin ne vaikuttavat merkittävästi virtauksen säätöpiirin suorituskykyyn. Tämä diagnoosi voidaan tehdä tässä työssä esitellyllä menetelmällä, joka tarvitsee vain vähän laskentatehoa ja jossa diagnosointi tapahtuu prosessia häiritsemättä (on-line). Näinollen menetelmä voidaan toteuttaa älykkääseen venttiilinohjaimeen.

Esitelty vikadiagnoosimenetelmä perustuu havaintoon, jossa vikaa lähin systeemin sisäinen muuttuja reagoi ja kompensoi vikaa takaisinkytketyssä säätöjärjestelmässä. Tämä johtaa myös siihen, että kaikkien vikaa edeltävien sisäisten muuttujien toimintapiste muuttuu vian seurauksena. Kun nämä toimintapistemuutoset voidaan havaita, voidaan myös systeemiin kohdistuvat viat diagnosoida. Esiteltyä menetelmää voidaan soveltaa kaikissa takaisinkytkettyä säätöä käyttävissä mekatronisissa järjestelmissä. Tämä esitelty menetelmä on verifioitu vikasimulaattorissa ja laboratoriossa koesarjoilla ja se pystyi diagnosoimaan kaikki testatut vikatapaukset.

Avainsanat vikasimulaattori, vian havaitseminen, diagnostiikka, prosessin säätöventtiili

ISBN (painettu) 978-952-60-4853-6 **ISBN (pdf)** 978-952-60-4854-3

ISSN-L 1799-4934 **ISSN (painettu)** 1799-4934 **ISSN (pdf)** 1799-4942

Julkaisupaikka Espoo **Painopaikka** Helsinki **Vuosi** 2012

Sivumäärä 75 **urn** http://urn.fi/URN:ISBN:978-952-60-4854-3

Preface

The research work for this thesis was done during 2009-2012 at Metso Automation Inc. I would like to thank my superiors Mika Kreivi and Sami Nousiainen and ex-superiors, Kari Hartikainen, Kaj Schlupp, and Sami Hakulinen, for this opportunity to learn and challenge myself within the postgraduate studies and research related to this thesis.

Professor Matti Pietola, as a supervisor, and Jouni Pyötsiä, as an advisor, deserve thanks for their valuable comments and support during this project.

This work has been partly supported by the 30th Anniversary Foundation of Neles Inc., which is gratefully acknowledged.

Finally, I would like to thank my wife Taija and children Matias and Maisa for their endless patience and support during these intensive years.

Helsinki, September 2012

Timo Manninen

Table of Contents

Symbols and abbreviations

m_f	effective mass of the flapper	[kg]
F_v	viscous damping force	[N]
F_c	coil force	[N]
F_s	flapper spring force	[N]
F_p	pressure force	[N]
P_{Pre}	prestage pressure	[Pa]
U	coil input voltage	[V]
ff	voice-coil force factor	[N/V]
T_a	ambient temperature	[K]
T_{ref}	voice-coil reference temperature	[K]
$Temp_{Coef}$	voice-coil temperature coefficient	
P_S	supply pressure	[Pa]
FPF_{Coef}	flapper pressure force coefficient	
$A_{nozzleEA}$	effective area of pressure at the nozzle	[m²]
A_{Pre}	flow area of the fixed restrictor	[m²]
A_{Nozzle}	flow area of the nozzle	[m²]
$\dot{m}$	mass flow	[kg/s]
A	flow area	[m²]
R	gas constant (287)	[J/kgK]
p_1	inlet pressure	[Pa]
T_1	inlet flow temperature	[K]
Ψ	flow function	
C_d	discharge coefficient	
p_2	outlet pressure	[Pa]
Γ	polytrophic constant (for an adiabatic process with air $\gamma = 1.4$).	
$\dot{m}_{net}$	net mass flow	[kg/s]
$\dot{m}_{in}$	mass flow through the fixed restrictor	[kg/s]
p	pressure	[Pa]
V	volume	[m³]

A_c	moving surface area of the volume change	[m²]
v	spool valve velocity	[m/s]
m_s	mass of the spool	[kg]
F_{ss}	spool spring force	[N]
F_{co}	control pressure force	[N]
F_{sp}	supply pressure force	[N]
F_d	diaphragm spring force	[N]
F_{fs}	friction force in the spool	[N]
k_{ss}	spool spring constant	[N/m]
x_s	spool position	[m]
x_{spre}	spool spring pretension	[m]
F_{dCoef}	diaphragm coefficient	
F_{dpre}	spring force caused by diaphragm at the prestage pressure end of the spool valve	[N]
F_{ds}	spring force caused by diaphragm at the spring end of the spool valve	[N]
F_f	friction force	[N]
ZV	zero velocity region	[m/s]
F_{Slip}	friction force when $v \neq 0$	[N]
F_{Stick}	friction force when $v = 0$	[N]
F_{cPos}	Coulomb friction force when $v > 0$	[N]
F_{vPos}	viscous friction coefficient when $v > 0$	
F_{sPos}	stiction force when $v > 0$	[N]
F_{cNeg}	Coulomb friction force when $v < 0$	[N]
F_{vNeg}	viscous friction coefficient when $v < 0$	
F_{sNeg}	stiction force when $v < 0$	[N]
F_e	external resultant force driving the spool valve	[N]
m_a	effective total mass of the piston and other moving parts	[kg]
F_{sa}	spring force	[N]
F_{fa}	friction force	[N]
F_{ap}	actuator pressure force	[N]
F_l	load force	[N]
P_{ac}	actuator pressure	[Pa]
Q	volumetric flow	[m³/s]
C_v	capacity coefficient	
dp	pressure difference over the valve	[bar]
dp_0	pressure difference over the valve when the valve is closed	[bar]

DP_f	pressure difference over the valve when it is fully open	[bar]
H	entropy	
P	probability	

FDD	fault detection and diagnosis
DUT	device under test
stiction	static friction
DAMADICS	Development and Application of Methods for Actuator Diagnosis in Industrial Control Systems
DCS	Distributed Control System
MVH	Multi-Variable Histogram

1. Introduction

1.1 Background

Safer, more reliable, and more profitable are continuous development topics in modern process plants. Therefore the early detection of faults and other problems concerning the process are required. This detection is usually performed by using fault detection and diagnosis (FDD) methods implemented in a condition monitoring system.

Condition-based maintenance as part of predictive maintenance is one of the tools used to increase productivity and reliability in the process industry. This is done by minimising unscheduled shutdowns and loss of product quality. Process plant performance and reliability cannot be improved without revealing deviations or problems by means of a condition monitoring system. This problem identification has to take place before problems become too serious in order to prevent major repairs and production breakdowns. Identification also has to take place online without disturbing the process, so as to maintain the efficiency of the plant. For this reason traditional offline performance tests are not feasible in real industrial applications these days.

Condition monitoring systems are typically centralised monitoring systems where intelligence is at the top level of the process plant, rather than at the field device level, as in distributed systems. When this centralised schematic is used, sensors also have to be installed to all the primary variables of the field devices, in addition to the process variables, to make field device faults observable. Otherwise these faults are not observable as a result of the control loop inside the field device compensating for them until some internal variable saturates and field device performance is affected. After field device performance is affected by the internal faults, these faults can also be detected through process variables. But then the detection happens too late to keep process performance at an optimal level and to have time to prepare repair work. Installing additional sensors into the field devices leads to very complicated

and expensive systems where deep expertise concerning the operation of the device is required from monitoring system designers. As a result of the complexity of these systems, faulty alarms are easily generated and maintaining such a system requires a lot of resources.

Ideally, intelligent autonomous devices can be part of a centralised condition monitoring system and can identify locally all the factors or the problems limiting the efficiency of the local process. This approach reduces the complexity of the condition monitoring system because the number of sensors, wires, and diagnosis loops connected to the monitoring system is reduced.

Manufacturers of intelligent devices have the best knowledge about these devices and they know the problems the devices can meet during operation. Therefore it is reasonable for device manufacturers to implement fault detecting and diagnosis features in intelligent devices, as opposed to the traditional top level-based condition monitoring systems.

As shown in Figure 1, process valves are fundamental components in the process industry. In a process plant there can be tens of thousands of manually operated valves and thousands of control valves. Many important process variables, such as flows and pressures, are controlled through these control valves. Therefore problems in control valves can cause significant process disturbances and influence the quality of the final product.

Thus control valves, as the most common final control element in the control loop in the process industry, have considerable potential to support predictive maintenance. For this reason they have to have FDD capabilities. Currently, valve controllers can detect some symptoms or faults, but not diagnose them. At the moment more detailed control valve performance analysis can be done by experts analysing offline test results such as hysteresis and step response test results. This is not an effective method for analysis, because the valve has to be isolated from the process to get these test results and analysis done. A more effective method is to perform the diagnosis online during the operation of the device without disturbing the process. Hence there is a need to research online methods to detect and diagnose typical control valve faults.

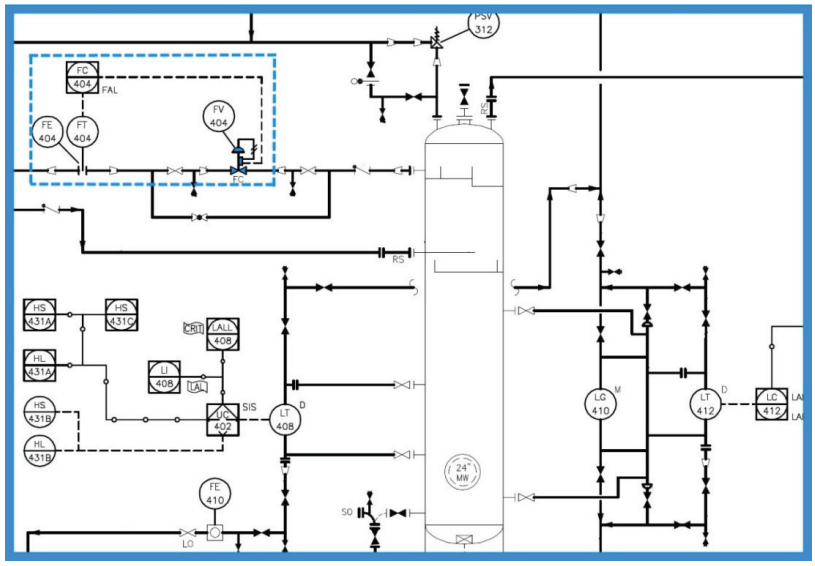

Figure 1. Control valve in flow control loop as part of a unit process.

In this study fault detection means recognising that a fault has occurred, while fault diagnosis means finding the cause and location of the fault. Advanced fault detection methods are based on signal and process models of the system. In these methods fault symptoms are generated through system theory methods and system models. Fault diagnosis methods use, among others, statistical decisions, artificial intelligence, and soft computing methods to form causal symptom-fault relationships.

1.2 Research problem

Nowadays valve controllers can detect some symptoms from the control valve without having the capability to pinpoint the real root cause of the fault or localise the problem. Diagnosing a fault correctly is essential in order to be able to allocate resources effectively to repair the cause of the fault. On the other hand, only information on which module or submodule has to be replaced to repair the problem is required when performing maintenance actions.

Many advanced FDD methods are presented in the literature, but implementing these methods in embedded systems is not possible in many cases because of limited computing power. This computing power is especially limited with valve controllers being installed in the intrinsically safe zones in process plants. Therefore energy in these devices is extremely limited in order to avoid the ignition of possible flammable gases in the

operating environment. Another challenge when researching FDD methods is getting data from the system being observed to develop and validate these methods. If a real process is used for data collecting, many faults are impossible to introduce in a system that is already running and fault simulations are restricted by the wish not to disturb the operation of the process. When a test bench in a laboratory is used to collect these data, problems are faced when implementing faults on the test bench and keeping the consequences of a fault repeatable over different test runs.

At the moment offline tests such as hysteresis and step response tests are used to evaluate control valve performance. This is not an effective method for analysis, because the valve has to be isolated from the process to run these tests. A more effective method is to perform the diagnosis online during the operation of the device without disturbing the process.

Finally, the research problem is to build an environment where fault detection and diagnosis methods can be researched effectively and after this to find or develop an online method to detect and diagnose specified control valve faults before there is a severe impact on flow control loop performance that is implementable in a valve controller.

1.3 Aim of the research

The objective of this research is online fault detection and diagnosis methods that are implementable in valve controllers.

1.4 Scope of the research

The scope of the research is fault detection and diagnosis methods for quarter-turn pneumatic control valves; sliding-stem valves are excluded. This control valve type represents the typical quarter-turn control valve used in the oil and gas industries.

When these methods are being researched, methods requiring low computing power must be preferred. This is essential when implementing these methods in embedded systems such as valve controllers. A low computing power method means in this study, the structure of the code is simple and amount of arithmetical operations are minimised. Especially floating point operations requires much computing power and therefore should be avoided.

Additionally, fault detection and diagnosis has to be done before there is a severe impact of the fault on flow control loop performance. That gives time to the maintenance organisation to schedule the maintenance actions that are required to prevent production breakdowns and loss of final product quality.

Only online FDD methods are considered in this research to perform diagnosis efficiently online during device operation without disturbing the process.

A specified set of typical control valve faults presented in Table 1 is considered in this research; for example, sensor faults are excluded from this research.

Table 1. Faults.

Module	Fault		
Nozzle-flapper	Obstruction in fixed restrictor	Obstruction in nozzle	Leakage
Spool valve	Friction change		
Actuator	Friction change	Leakage	Mechanism backlash
Valve	Friction change		

1.5 Research methods

Literature related to the control valve modelling and the control valve fault detection and diagnosis was studied for the *State of the art* section.

In the fault simulator, a physics-based analytical modelling was utilised to make physical fault modelling and fault location in the model feasible. Additionally, analytical modelling also gives knowledge about the system and helps to understand the behaviour and characteristics of the system. This is valuable when considering the fault detection and diagnosis methods for the system. The derived models were fitted with some nonlinear fitting parameters, such as position-related spring coefficients. That required many experiments which were conducted in the laboratory to get the estimation data from the system. The models were implemented in the Matlab Simulink™ environment and solved with numerical methods.

Four different fault simulation schemes were run in the simulator with all faults (presented in Table 1) to research the impact of faults on the system in different valve use cases.

An online fault detection and diagnosis method was developed that was based on the fault simulation data. The method was verified with the simulator and test bench runs (emulations).

1.6 Contribution

The contributions of this study are:

- fault simulator for quarter-turn pneumatic control valve
- fault detection and diagnosis method implementable in a valve controller

Compared to the other studies in these fields, the aspect of the valve controller is considered in all related matters and the quarter-turn valve design is utilised as the opposite of the sliding-stem design.

It has been possible to analytically model control valve dynamics, despite their inherent nonlinearities for the fault simulator. These nonlinearities of the system have been identified and estimated through selected fitting parameters. The models that were derived have been verified with measurements and the modelling error is found to be acceptable for the fault simulations. Some typical control valve faults have been simulated and impacts on the internal variables of the flow control loop and control performance analysed. The fault simulator presented here can be used for fault detection and diagnosis, as well as robust control research.

On the evidence of simulations and test bench test runs, it is possible to detect and diagnose typical control valve faults before there is a severe impact on flow control loop performance. This can be done with the online method requiring low computing power that is introduced in this study. This means the method is implementable in a valve controller and diagnosis can take place without disturbing the process. The method introduced here is based on the observation that the internal variable closest to the fault compensates and reacts to the fault first when feedback control is utilised. That leads to an operation point shift for all the internal variables before a fault in the chain of internal variables in the system. This principle can be utilised in all feedback-controlled mechatronic systems. The fault detection and diagnosis method introduced here was verified with simulator and test bench runs and found to be applicable to the detection and diagnosis of all the faults that were tested.

1.7 Structure of the thesis

This thesis consists of six chapters. Their contents are briefly summarised below.

Chapter 2 introduces literature related to this study. Section is divided according to two main themes of this study, the control valve fault simulator and the control valve fault detection and diagnosis.

Chapter 3 explains in detail the control valve fault simulator. It is based on analytical models and is implemented in the Matlab Simulink™ environment. The simulator was verified with test bench measurements in the laboratory. After this the simulator was used for fault simulations to generate data for FDD research.

Chapter 4 presents an online fault detection and diagnosis method that was based on fault simulation data. The method is implementable in embedded systems and the method was verified with simulator and test bench runs.

Chapter 5 concludes this study and presents next research steps.

2. State of the art

This chapter introduces relevant literature related to this study. The section is divided according to two main themes of this study, the control valve fault simulator and the control valve fault detection and diagnosis.

2.1 Control valve fault simulator

The fault simulator presented in this study consists of the following models: a valve controller (e.g. nozzle-flapper and spool valve), a pneumatic spring return cylinder actuator, a segment-type process control valve, medium flow in the process pipe, the flow control loop, and faults as shown in Figure 2. The fault simulator was introduced for the first time by the author in the reference (Manninen T., 2011).

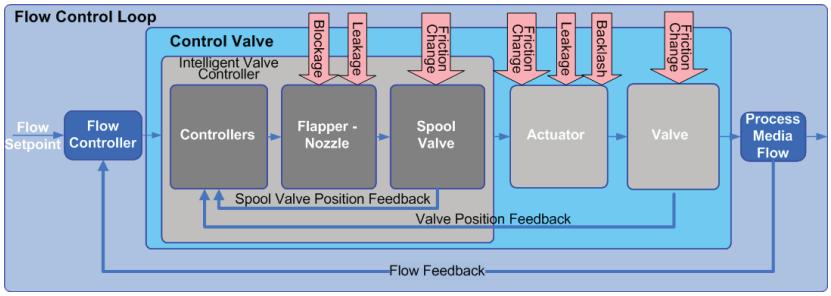

Figure 2. Control valve in flow control loop and modelled faults (red arrows).

All the modules of a quarter-turn control valve have been modelled to varying degrees in the literature. Most of the research activities have been in the field of pneumatic actuator models. A thermodynamic process including heat exchange and friction has been the main topic in these papers. There are no detailed valve controller models available, but models of the pneumatic pre- and output-stage components (nozzle-flapper and spool valve) of valve controllers are available. Process control valve modelling has concentrated mainly on sliding-stem valves with linear-type

actuators, as opposed to the quarter-turn designs that are the object of this study. A detailed valve controller model is introduced in this study.

Next, references related to the fault simulator domain are briefly introduced.

2.1.1 Prestage (nozzle-flapper) models

In the field of prestage modelling one of the early papers is (Burrows C. R., 1977). In that paper a complete model of the nozzle-flapper is presented. The paper concentrates on the effects of flow force for nozzle-flapper dynamics and therefore an experimental flow force equation is presented in the paper.

Another paper that considers the flow force in particular is introduced by (Wang T., 2005). In that paper a complete model for the nozzle-flapper is also presented.

(Kagawa, 1985) introduced a dimensionless flapper-nozzle model and the effect of heat transfer in the nozzle-flapper is considered as well.

It should be noted that the construction of the nozzle-flapper in these references includes nozzles on both sides of the flapper, while the construction used in this study includes only one nozzle on one side of the flapper.

2.1.2 Spool valve and actuator models

(Shearer, 1956) introduced the first pneumatic actuator and the spool valve model as part of a complete pneumatic servo system model. In his subsequent papers (Shearer, 1956) and (Shearer, 1957), load mass and other nonlinearities such as Coulomb friction were added to the linear model presented in the first paper.

A spool valve model based on the ISO 6358 standard (anon., 1989) is presented by (Virvalo, 1995) as part of a pneumatic servo system model. In the model the actuator model is based on the adiabatic process and an ideal gas model.

Another spool valve model based on an ISO standard is introduced by (Mare J.-C., 2000), again as part of a pneumatic servo system. In that reference heat transfer and friction are especially considered in the actuator model.

(Richer E., 2000) presented a detailed mathematical model of a dual-action pneumatic actuator controlled by means of proportional spool valves. In the spool valve model the effects of nonlinear flow through the spool valve were researched. Air compressibility in the cylinder chambers,

leakage between chambers, and time delay and attenuation in the pneumatic lines were carefully considered in the actuator model as well.

An actuator model that took into account the real gas behaviour and the thermal time constant for estimating heat transfer was introduced by (Heras, 2003).

(Sorli M., 2009) investigated the effect of the heat exchange process on the characteristics of pneumatic actuators and their pneumatic stiffness.

2.1.3 Control valve models

(Pyötsiä, 1991) introduced a nonlinear mathematical model of a quarter-turn pneumatic control valve consisting of these models: a valve positioner, actuator, process valve, and pipeline flow.

A sliding-stem control valve model is presented by (Bartys M., 2006). There the same kind of fault simulator concept is used for fault detection and diagnosis research as in this study.

2.1.4 Actuator friction models

(Schroeder L. E., 1993) researched sliding friction forces in a pneumatic actuator. In this study seven different friction models were validated with experiments.

The friction force between an elastomeric seal and a pneumatic cylinder was evaluated by (Raparelli T., 1997) through experiments and numerical simulations.

2.1.5 Process valve friction models

(Garcia, 2007) introduced a method for the offline identification of three Karnopp friction model parameters and two system parameters for sliding-stem control valves.

(Romano R. A., 2007) compared two Karnopp friction model parameter estimation methods for sliding-stem control valves. The method was the same as that presented in the previous reference (Garcia, 2007).

(Garcia, 2008) compared eight different friction model simulation results to test bench results. Again, the tests and simulations were performed with sliding-stem control valves.

2.1.6 Control valve static friction (stiction)

(Kano M., 2004) introduced a stiction model including two parameters.

(Choudhury M. A. A. S., 2005) proposed a definition of stiction and introduced a data-driven model for stiction.

A stiction model accounting for valve input rate was presented by (Srinivasan R., 2008).

(Zhi Xiang Ivan L., 2009) proposed a Hammerstein stiction model including only one parameter.

2.2 Control valve fault detection and diagnosis

Valve controllers can detect some faults or symptoms, but cannot diagnose them. This detection is usually based on simple methods such as limit or trend checking. In steady state conditions these methods can be reliable, but when the operating point of the system changes and an alarm limit is set that is related to this operating point only, false alarms are easily generated.

Fault detection methods have developed, starting from the limit and trend checking-based methods to the advanced model-based algorithms including analytical redundancy, parity equations, state observers, unknown input observers, and parameter estimations. These advanced methods are based on a model of the system being monitored. The goal within these methods is to generate symptoms that react only to faults in the system being monitored. These symptoms can be based, for example, on the difference between the model outputs and corresponding measured sensor signals from the system being monitored. A common requirement for all these advanced methods is knowledge of the system and being able to model the system. An additional requirement is the need for high computing power to run these models or estimate model parameters. When symptoms such as residuals or parameter/state variable changes react to the faults, the next step is to find a method to diagnose the fault. These diagnosing methods use, among others, statistical decision, artificial intelligence, and soft computing methods to form causal symptom-fault relationships.

The most active research area in control valve diagnostics has been the diagnosis and compensation of static friction (stiction), because stiction is a common root cause of flow control loop oscillation in process plants. Almost all the approaches to the diagnosis of stiction have been made from the point of view of distributed control systems (DCS), not from field devices. This means that only process variables are used for diagnosis and methods are run on the DCS level.

The DAMADICS benchmark problem (Bartys M., 2006) has inspired many papers in the field of control valve diagnostics. These papers mostly deal with soft computing methods such as neural networks and fuzzy systems or combinations of these.

Next, references related to the domain of the detection and diagnosis of control valve faults are introduced.

(Deibert, 1994) studied an observer-based FDD scheme in a flow control loop that included a sliding-stem control valve. The faults considered in the study were increased friction in the stuffing box and changes in the effective flow area in the valve. Control performance indices and valve position-based estimates were used as symptoms. Process variables were used as inputs to the FDD strategy. The method was verified by simulations and real process runs.

Typical control valve faults and failure rates are introduced by (McGhee J., 1997). These typical faults in a sliding-stem valve are mentioned as being, for example, internal and external leakage and scoring of the valve plug and seat. Additionally, artificial neural networks were applied to estimate actuator shaft output torque as a model-based fault detection method.

(Sharif M. A., 1998) reviewed commercial diagnostic software with simulation in the laboratory of actuator vent hole blocking and crystallisation around the valve plug. The diagnostic software was not able to diagnose these faults. All the diagnosis was carried out on the basis of offline performance tests, such as hysteresis and step response tests. In the study it was stated that by combining several separate test results, more precise diagnostic results can be achieved. In his second paper, (Sharif M. A., 1999) he studied the effects of several faults on the sliding-stem control valve. The faults that were considered were: gradual blockage of the actuator vent hole, a damaged valve stem, and damaged valve stem packing rings. In the study external sensors were used to monitor the system. These sensors measured pressure, mass flow, displacement, and temperature. Diagnosis was done with a valve hysteresis test and signal-based methods. The diagnosis results were verified with laboratory measurements. In his third paper (Sharif M. A., 2000), he proposed an expert software system for analysing the results obtained with commercial diagnostic software. The results were based on offline valve hysteresis and step response tests, as in his previous papers. In the study a sliding-stem control valve was used and the effects of several faults at one time on control valve performance were considered. The faults considered in the study were gradual blockage of the actuator vent hole, a damaged valve stem, and damaged valve stem packing rings.

(Kayihan A., 2000) introduced a state space sliding-stem control valve model in order to utilise an advanced nonlinear model predictive control strategy to compensate for the effects of friction. An observer-based fault detector and fault diagnosis based on a fault tree are also discussed.

Observer parameter estimation is used for diagnosis as well. This means that the method can be run online. In the study it is stated that the method that was developed is computationally too intensive to implement in a valve controller.

(Balle P., 2000) studied FDD in a pilot plant in a flow control loop with six faults. The faults in the flow control loop were an air leak in the pipe, stuffing box friction, a flow sensor fault, partial clogging of the valve, erosion of the valve plug, and a fault in the valve position controller. The FDD scheme that was utilised was based on fuzzy models and ran online. Six symptoms were generated, such as output error in the model and real process, control performance indices, and model parameter errors. These symptoms were evaluated with a fuzzy classification tree. Only the process flow control loop variables, such as flow set point, valve set point, and flow measurement signal, were used as inputs in this FDD scheme.

(Karpenko M., 2003) researched sliding-stem control valve fault detection. The faults that were considered were incorrect supply pressure, actuator vent blockage, and diaphragm leakage. Fault detection and diagnosis were performed by a neural network-based classifier. The above-mentioned faults were experimentally introduced to the control valve and data for classifier training were obtained directly from the standard software that came with the control valve. All the faults that were being researched with various levels of magnitude were detected and diagnosed. The drawback of this method is that offline performance tests, such as valve hysteresis and the step response test, have to be run to obtain input data for the FDD method.

2.2.1 DAMADICS benchmark problem

Most of the FDD methods researched in academic papers require data from faulty process states and these are not available for industrial implementations. This was noticed and a new benchmark problem was introduced to find methods for the industry to implement the methods without having analytical knowledge of the actuator or system or faulty states of the system. This benchmark is called DAMADICS (Development and Application of Methods for Actuator Diagnosis in Industrial Control Systems) and was introduced by (Bartys M., 2006). In the benchmark problem three sliding-stem control valves were modified mechanically and electronically to simulate faults in the sugar juice process in a sugar factory. A total of 19 incipient or abrupt faults were introduced into the process and a system model was built for the benchmark problem. These faults were located in all the main modules of the system, including the process valve, actuator, and positioner. For benchmarking purposes five measurements

and one control signal are considered. These signals are the control valve set point, valve inlet pressure, valve outlet pressure, valve stem displacement, liquid flow rate, and liquid temperature. Only single fault scenarios were considered in this benchmark.

This benchmark problem has inspired numerous FDD papers related to sliding-stem control valves. These papers mostly deal with soft computing methods such as neural networks and fuzzy systems. Other model-based methods such as signal or process model-based methods have not been widely researched. Neural networks or fuzzy methods are usually used to avoid complex analytical nonlinear system modelling. When these black box modelling methods are used the inner structure of the model cannot be used for FDD purposes and the faults have to be taught to the monitoring system. Additionally, these soft computing methods are computationally intensive, preventing the implementation of these methods in valve controllers to achieve the distributed monitoring system scheme discussed earlier.

Next, references related to the DAMADICS benchmark problem are briefly introduced.

(Calado J.M.F., 2006) introduced a fuzzy neural network-based FDD method and several faults at a time were considered in the study. (Puig V., 2007) proposed a nonlinear neural network model to implement a robust fault detection method. Another robust approach was studied by (Mrugalski M., 2008). There neural network model uncertainty is used to create robust FDD.

A neuro-fuzzy FDD method using the system parameters as residuals was presented by (Uppal F. J., 2002). Other neuro-fuzzy methods were introduced by (Patton, 2005), (Uppal F. J., 2006), and (Korbicz J., 2007).

Fuzzy sets are used to describe the relationship of the current state of the system to the normal or faulty state. This can be done through encoding expert knowledge in verbal form using if-then rules to make the FDD model.

(Bartys M. Z., 2002) introduced four fuzzy-based fault diagnosis methods applicable for embedded systems in terms of a low computing power requirement. The valve controller set point, control current of the EP transducer, actuator pressure, stem displacement, and media flow rate were used as inputs in these methods. (Várkonyi-Kóczy A. R., 2003) presented an anytime fuzzy-based FDD approach. Anytime means the method can provide FDD results regardless of the time and resources available for FDD computation. This is an important factor when one is considering online FDD methods implemented in embedded systems. Another computational

cost-related reference is (Baranyi P., 2004). There the trade-off between the fitting of the fuzzy model and computational cost was considered.

(Bocănială C. D., 2006) introduced a fuzzy-based FDD method. This method was verified with all the faults introduced in the benchmark and with 20 different strength levels. (Mendonca L.F., 2009) utilised fuzzy models for fault detection and residuals for diagnosis.

In principal component analysis (PCA) the target is to extract correlated variables to reduce the dimensionality of the system being monitored. This approach to FDD was used by (Mina J., 2005).

(Ling B., 2007) proposed a signal model-based method. In this method geometric features of measured signals are extracted and compared to the features of the normal state of the system. The flow set point, flow, and valve set point are used as input signals. The faults considered are dead-band, backlash, leakage, and blocking. The method is utilised online and is used in steady states.

3. Control valve fault simulator

In this chapter is explained in detail developed control valve fault simulator. It is based on analytical models and is implemented in the Matlab Simulink™ environment. The simulator is verified with the test bench measurements done in the laboratory. After this the simulator was used for fault simulations for generating data for FDD research.

The fault simulator consists of the following models: a valve controller (nozzle-flapper and spool valve), a pneumatic spring return cylinder actuator, a segment-type process control valve, medium flow in the process pipe, and the flow control loop as seen in Figure 2. These analytical models are fitted with some nonlinear fitting parameters, such as position-related spring coefficients. A physics-based analytical model scheme was chosen to make physical fault modelling and fault location in the model feasible. Some relevant faults for each component are modelled to make fault impact simulations possible. In the fault simulator different fault cases can be simulated and their consequences analysed.

The simulator simulates the operation of a quarter-turn pneumatic control valve. It consists of a valve controller (nozzle-flapper and spool valve), a pneumatic spring return cylinder actuator, and a segment-type process control valve as presented in Figure 3. In the figure, the internal variables of the system and causalities of the variables are presented to describe system operation.

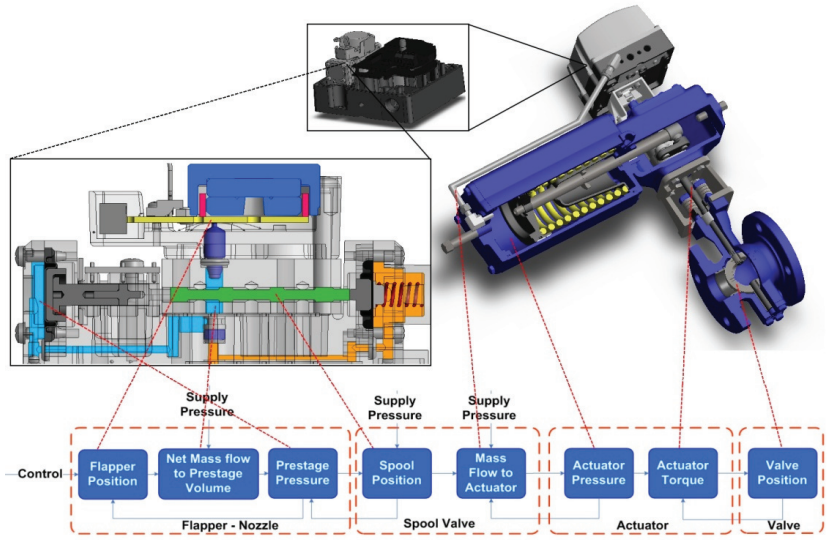

Figure 3. Control valve and its internal variables.

3.1 Control valve model

The analytical modelling scheme was chosen to make physical fault modelling and fault location in the system easy. Additionally, analytical modelling also gives knowledge about the system and helps to understand the behaviour and characteristics of the system. This is valuable when considering fault detection and diagnosis methods for the system.

In the modelling, the primary target was to model the main causalities and the static and dynamic properties of the system. The target was not to estimate all the parameter values or make a general model for all possible control valves.

The submodels of the analytical control valve model are presented below.

3.1.1 Nozzle-flapper model

The nozzle-flapper is used as a prestage of the pneumatic system in the control valve considered in this study. In the nozzle-flapper system presented in Figure 4, the prestage pressure P_{Pre} can be controlled by adjusting the flapper position, which controls the flow from the prestage volume. This prestage pressure P_{Pre} controls the position of the spool valve.

An equation of motion for the flapper (1) is derived from Figure 4.

$$m_f\ddot{x} + F_s + F_v + F_c - F_p = 0 \qquad (1)$$

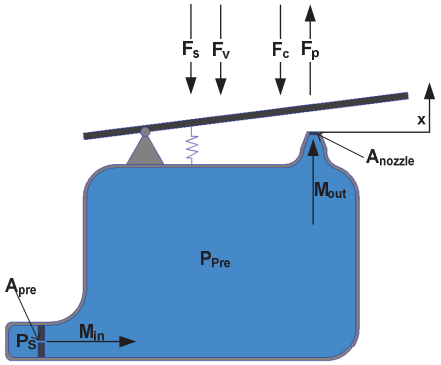

Figure 4. Nozzle-flapper schematics.

Here m_f is the effective mass of the flapper [kg], F_v the viscous damping force [N], F_c the coil force [N], F_s the flapper spring force [N], and F_p the pressure force [N].

F_c is introduced in Equation (2). This force is linearly related to the coil input voltage and is produced by a voice-coil which is attached to the flapper.

$$F_c = U * ff * ((T_a - T_{ref}) * Temp_{Coef} + 1) \quad (2)$$

Here U is the coil input voltage [V], ff is the voice-coil force factor [N/V], T_a is the ambient temperature [K], T_{ref} is the voice-coil reference temperature [K], and $Temp_{Coef}$ is the voice-coil temperature coefficient.

F_p is introduced in Equation (3) and is caused by the effect of the prestage pressure P_{Pre} through the nozzle and the flow adjacent to the flapper. P_S [Pa] denotes the supply pressure in Figure 4.

$$F_p = FPF_{Coef} * P_{Pre} * A_{nozzleEA} \quad (3)$$

Here FPF_{Coef} is the flapper pressure force coefficient, P_{Pre} is the prestage pressure [Pa], and $A_{nozzleEA}$ is the effective area of the prestage pressure at the nozzle [m²].

Equations (4) and (5) are used to model mass flows through the fixed restrictor A_{Pre} and the nozzle A_{Nozzle} shown in Figure 4. These equations are based on an adiabatic process, ideal gas law, and zero upstream velocity.

$$\dot{m} = A\Psi p_1 C_d \sqrt{\frac{2}{RT_1}} \quad (4)$$

Here $\dot{m}$ is the mass flow [kg/s], A the flow area [m²], R the gas constant 287 J/kgK, p_1 the inlet pressure [Pa], T_1 the inlet flow temperature [K], Ψ the flow function, and C_d the discharge coefficient. Ψ is given by Equation (5) and depends on the pressure ratio $\frac{p_2}{p_1}$.

$$\Psi = \begin{cases} \sqrt{\left[\frac{\gamma}{\gamma-1}\left\{\left(\frac{p_2}{p_1}\right)^{\frac{2}{\gamma}} - \left(\frac{p_2}{p_1}\right)^{\frac{1+\gamma}{\gamma}}\right\}\right]}, & \frac{p_2}{p_1} > \left(\frac{2}{\gamma+1}\right)^{\frac{\gamma}{\gamma-1}}, \ subsonic\ flow \\ \left(\frac{2}{\gamma+1}\right)^{\frac{1}{\gamma-1}}\sqrt{\frac{\gamma}{\gamma+1}}, & \frac{p_2}{p_1} \leq \left(\frac{2}{\gamma+1}\right)^{\frac{\gamma}{\gamma-1}}, \ choked\ flow \end{cases} \quad (5)$$

Here p_2 is the outlet pressure [Pa] and γ the polytrophic constant (for an adiabatic process with air, γ = 1.4).

The net mass flow $\dot{m}_{net}$ to the prestage volume is introduced in Equation (6) and builds up the pressure P_{Pre} shown in Figure 4.

$$\dot{m}_{net} = \dot{m}_{in} - \dot{m}_{out} \quad (6)$$

Here $\dot{m}_{net}$ is the net mass flow [kg/s], $\dot{m}_{in}$ is the mass flow through the fixed restrictor [kg/s], and $\dot{m}_{out}$ is the mass flow through the nozzle [kg/s]. $\dot{m}_{in}$ and $\dot{m}_{out}$ are based on Equations (4) and (5).

Equation (7) is used to model the pressure P_{Pre}. In this equation an adiabatic process and ideal gas law are also assumed.

$$\dot{p} = \frac{\gamma}{V}(\dot{m}RT_0 - pA_c v) \quad (7)$$

Here p is the pressure [Pa], V the volume [m3], A_c the surface area of the volume change [m²], and v the velocity [m/s] of A_c. In this case $\dot{m} = \dot{m}_{net}$.

3.1.2 Spool valve model

A spool valve is used as an output stage of the pneumatic system in the control valve considered in this study. The position of the spool valve is controlled by the prestage pressure P_{Pre} formed in the nozzle-flapper system. The spool valve adjusts the actuator pressure and in this way the position of the process valve.

An equation of motion (8) for the spool is derived from

Figure **5**.

$$m_s\ddot{x} + F_{ss} + F_{fs} + F_d + F_{sp} - F_{co} = 0 \quad (8)$$

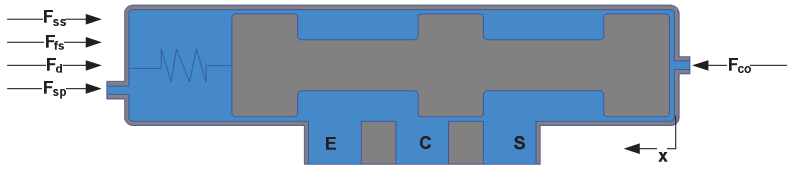

Figure 5. Spool valve schematics.

Here m_s is the mass of the spool [kg], F_{ss} the spool spring force [N], F_{co} the control pressure force [N], F_{sp} the supply pressure force [N], F_d the diaphragm spring force [N], and F_{fs} the friction force [N]. E stands for Exhaust, C for Cylinder, and S for Supply in the figure. Flow forces are not considered in this model.

The spool spring force F_{ss} is introduced in (9).

$$F_{ss} = k_{ss} * (x_s + x_{spre}) \tag{9}$$

Here k_{ss} is the spool spring constant [N/m], x_s is the spool position [m], and x_{spre} is the spool spring pretension [m].

The diaphragm spring force F_d is introduced in Equation (10).

$$F_d = F_{dCoef} * (F_{dpre} - F_{ds}) \tag{10}$$

Here F_{dCoef} is the diaphragm coefficient, F_{dpre} is the spring force [N] caused by the diaphragm at the prestage pressure end of the spool valve, and F_{ds} is the spring force [N] caused by the diaphragm at the spring end of the spool valve.

The friction model is an extended Karnopp model (11). In the original Karnopp model (Karnopp, 1985) parameters are common for both directions of movement. The extended model applied in the present work uses separate parameters for both directions of movement. Adding separate parameters was essential to achieve sufficient model fitting in the actuator model. There especially the Coulomb forces were notably different for the negative and positive directions of movement.

$$F_f = \begin{cases} F_{Slip} = \begin{cases} F_{cPos} + F_{vPos}v, & v \geq ZV \\ -F_{cNeg} + F_{vNeg}v, & v \leq ZV \end{cases} \\ F_{Stick} = \begin{cases} \min(F_e, F_{sPos}) \\ \max(F_e, -F_{sNeg}) \end{cases} \quad |v| < ZV, \quad \begin{matrix} F_e \geq 0 \\ F_e \leq 0 \end{matrix} \end{cases} \tag{11}$$

Here F_f is the friction force [N], v is the spool valve velocity [m/s], ZV is the zero velocity region [m/s], F_{Slip} is the friction force [N] when $v \neq 0$, and F_{Stick} is the friction force [N] when $v = 0$. F_{cPos} is the Coulomb friction force [N] when $v > 0$. F_{vPos} is the viscous friction coefficient when $v > 0$, F_{sPos} is the stiction force [N] when $v > 0$. F_{cNeg}, F_{vNeg}, and F_{sNeg} are the corresponding forces for negative spool velocity. F_e is the external resultant force [N] driving the spool valve. Inside the ZV region the velocity is assumed to be zero and the friction force holds the spool valve in position until breakaway friction is overtaken.

Mass flow through the spool valve is modelled with the same mass flow equations (4) and (5) as within the nozzle-flapper. Leakage flow over the spool is not considered in this model.

3.1.3 Pneumatic spring return actuator model

The equation of motion (12) for the actuator piston is derived from Figure 6.

$$m_a\ddot{x} + F_{sa} + F_{fa} + F_l - F_{ap} = 0 \tag{12}$$

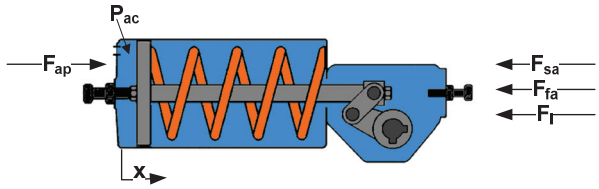

Figure 6. Pneumatic spring return actuator schematics.

Here m_a is the effective mass of the piston and other moving parts [kg], F_{sa} the spring force [N], F_{fa} the friction force [N], F_{ap} the actuator pressure force [N], and F_l the load force caused by the process valve [N]. The friction force model is the same extended Karnopp model (11) as used with the spool valve. The actuator pressure P_{ac} producing F_{ap} is modelled with the same equation (7) as in the nozzle-flapper. Leakage flow over the piston is not considered in this model.

3.1.4 Segment process control valve model

A process valve is fitted to the actuator with its shaft attached to the actuator hub, as shown in Figure 3. Consequently a separate equation of motion for the valve is not implemented and only the moment of inertia and friction are considered in the valve model. The friction model utilised is the same extended Karnopp model (11) as used with the spool and with the actuator.

3.1.5 Controller models

A cascade control scheme was implemented in the valve controller model. The outer loop controls the process valve position and the inner loop the spool valve position. The process valve position feedback control was implemented as proportional control, while the inner slave loop was implemented as PID control.

3.1.6 Medium flow in process pipe model

Flow through the process valve is modelled with Equation (13).

$$Q = 0.865 * C_v\sqrt{dp} \tag{13}$$

Here Q is the volumetric flow [m3/s], C_v is the capacity coefficient, and dp the pressure difference over the valve [bar]. dp is obtained from Equation (14) (Driskell, 1983). This equation models the pump and pipe characteristics by approximating both the characteristics of a centrifugal pump and the pressure drop in a pipe resulting from turbulent flow. This equation is only valid for liquids.

$$dp = dp_0 \frac{DP_f}{DP_f + (1 - DP_f)C_v^2} \tag{14}$$

Here dp_0 is the pressure difference [bar] over the valve when the valve is closed and DP_f the pressure difference [bar] over the valve when it is fully open.

3.1.7 Flow control loop model

The flow controller shown in Figure 2 is modelled as a PI feedback controller. In a real application the set point of this controller would come from the process control system.

3.1.8 Modelled faults

Eight typical control valve faults presented in Table 1 were modelled in the flow control loop model shown in Figure 2. The faults are clarified in more detail below.

- An obstruction in the fixed restrictor reduces flow through the fixed restrictor.
  The fault was modelled as a blockage coefficient affecting mass flow through the fixed restrictor.
- An obstruction in the nozzle reduces flow through the nozzle.
  The fault was modelled as a blockage coefficient affecting mass flow through the nozzle.
- A nozzle-flapper leakage (prestage pressure leakage) fault causes a reduction in the net mass flow to the prestage volume.
  The fault was modelled as a leakage path to the environment from the prestage volume.
- A spool valve friction change fault causes an increase in Coulomb, viscous, and static friction in the spool valve.
  The fault was modelled as a friction fault coefficient affecting the nominal friction parameter values.
- An actuator friction change fault causes an increase in Coulomb, viscous, and static friction in the actuator.
  The fault was modelled as a friction fault coefficient affecting the nominal friction parameter values.
- An actuator leakage fault causes a reduction in the net mass flow to the actuator.
  The fault was modelled as a leakage path to the environment from the actuator cylinder.
- An actuator mechanism backlash fault affects the actuator mechanism, transforming linear piston movement to rotary valve movement.
  The fault was modelled with a standard Simulink™ backlash block affecting the actuator piston movement before the transformation block.
- A valve friction change fault increases Coulomb, viscous, and static friction in the valve.
  The fault was modelled as a friction fault coefficient affecting the nominal friction parameter values.

3.2 Parameter estimations and model verification

The models presented above were implemented in the Matlab Simulink™ environment, as shown in Figure 7, and solved with numerical methods. Most of the parameters were fixed but some were chosen as fitting parameters. The fitting parameters were estimated manually for one model module (e.g. flapper equation of motion) at a time. With this approach possible nonlinearities of the fixed parameters will also be included in the fitting parameter. This is acceptable, because the motivation for the simulator is to model system causalities and performance, not to estimate exact parameter values.

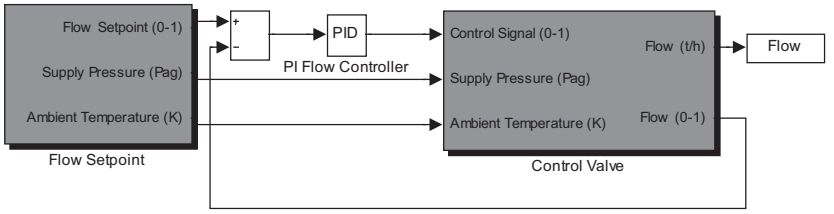

Figure 7. Implemented Simulink™ model.

Ramps as excitation signals were used to estimate the static properties of the module in its input-output domain, shown in Figure 8. Dynamic properties were estimated in the time domain with step-like excitation signals, as also shown in Figure 8. All the estimations were performed at three different supply pressure levels, for example, 0,3, 0,5, and 0,8 MPa, to obtain supply pressure-related nonlinearities in the model.

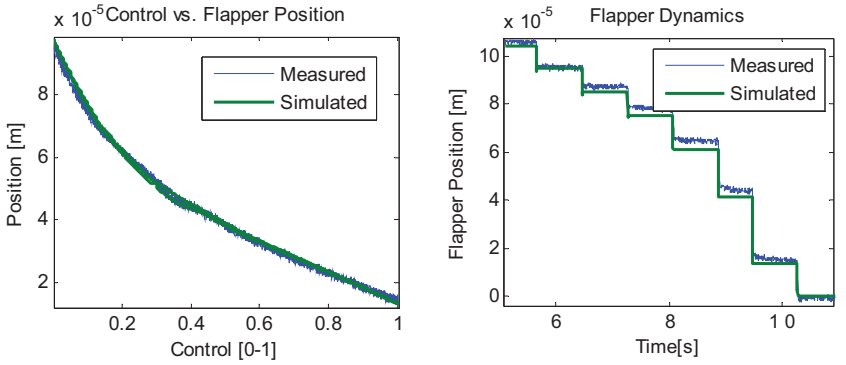

Figure 8. Flapper's input-output domain (left) and time domain (right).

The control valve was instrumented as shown in Figure 9 to measure the internal variables presented in Figure 3 in order to get data for parameter estimations and model verification. All internal variables except the net mass flow to the prestage volume were available through the dSPACE™ environment. In Figure 9 the labelled sensors are: (1) the laser sensor used to measure the flapper position; (2) the pressure sensor used to measure the prestage pressure; (3) the laser sensor used to measure the spool valve position; (4) the mass flow meters (two in number) used to measure the mass flow to and from the cylinder; (5) the pressure sensor used to measure the actuator pressure; (6) the strain gauge used to measure the valve load torque, and (7) the incremental encoder used to measure the process valve position, while label (8) stands for the valve seal loading device used for increasing the valve load.

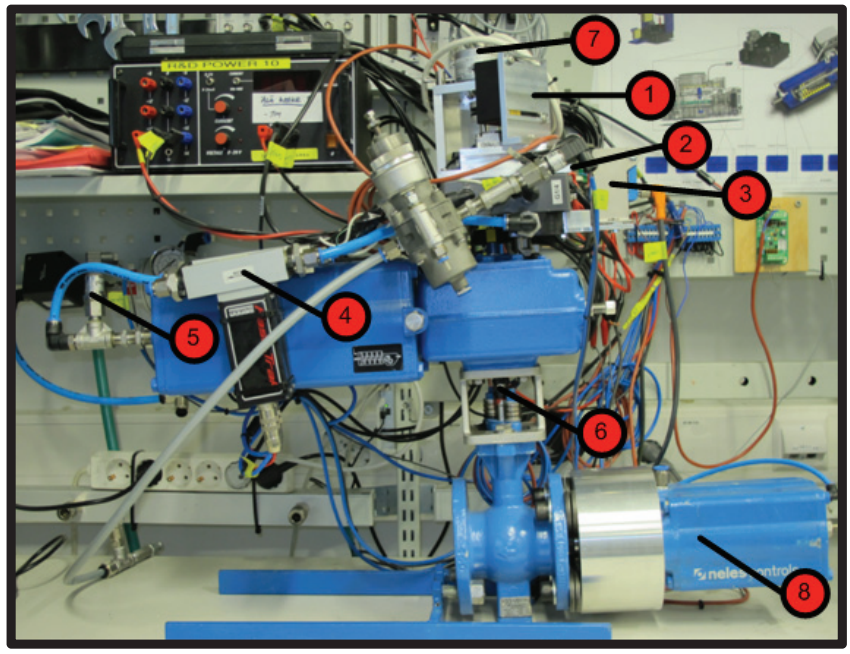

Figure 9. Test bench and external sensors.

3.2.1 Nozzle-flapper

The first estimated parameter in the flapper equation (1) was the flapper spring force F_s, representing the flapper spring coefficient. This lookup table was estimated by driving the flapper without supply pressure to introduce all the nonlinearities of the flapper spring force F_s and the voice coil force F_c (2). The simulated flapper spring force is shown in Figure 10. The red line

in the figure is a linear approximation of the lookup table data. When the linear approximation and simulation results are compared, it can be noticed that the voice-coil and flapper spring do not bring any significant nonlinearity to the system. Therefore in fault simulator-type models linear approximation can be considered to simplify the model.

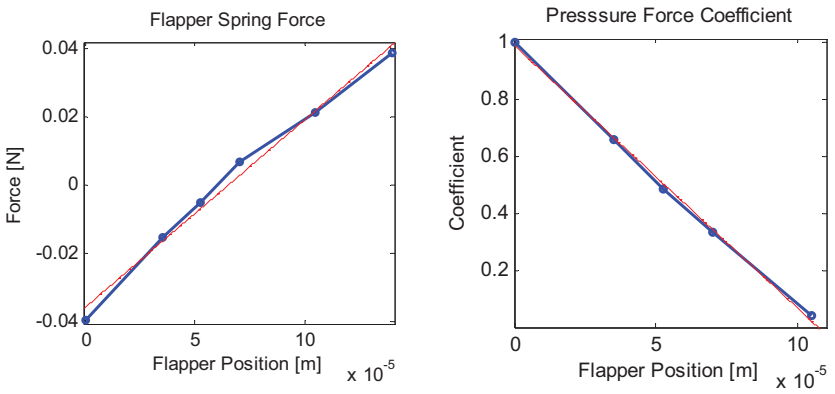

Figure 10. Flapper spring force (left) and pressure force coefficient (right).

The second estimated parameter in the flapper model (1) was the prestage pressure force coefficient FPF_{Coef} in Equation (3). Within this parameter the rest of the nonlinearities of the flapper model were obtained. That was done by driving the control signal ramps up and down and measuring the flapper position with three different supply pressures, 0,3, 0,5, and 0,8 MPa, connected to the prestage module.

Because of the flow between the flapper and the nozzle end, as presented in Figure 11, the effective area of the pressure force widens over the inner diameter of the nozzle. The effective area diameter was fitted to make the pressure force coefficient equal to one when the flapper is close to the nozzle.

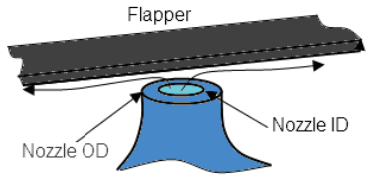

Figure 11. Flow in nozzle-flapper.

As can be seen from Table 2, the voice-coil force is not able to close the flapper tightly against the nozzle as a result of the pressure force. The pressure effect area $A_{nozzleEA}$ was estimated to be:

$$A_{nozzleEA} = \pi * \frac{(Nozzle_{ID}+0.4125*(Nozzle_{OD}-Nozzle_{ID}))^2}{4} \quad (15)$$

The estimated $A_{nozzleEA}$ agrees well with the result presented in the reference (Burrows C. R., 1977), where the pressure effect area can vary, depending on whether the area is calculated on the basis of the inner or outer diameter of the nozzle.

Estimated FPF_{Coef} lookup tables are shown in Table 2. The lookup table presented in Figure 10 is an average of the estimated tables shown in the table below.

Table 2. Estimated prestage pressure force coefficient lookup tables. 'N/A' means not available because of flapper movement range in the conditions being considered.

Flapper Position [mm]	0	0.0350	0.0525	0.0700	0.1050	Range [mm]
0,2MPa	0.9539	0.5846	0.4000	0.2550	N/A	0.005-0.075
0,5MPa	1.0462	0.6769	0.5046	0.3525	0.0492	0.015-0.100
0,8MPa	N/A	0.7076	0.5538	0.4000	0.0308	0.030-0.105

In Figure 10 the force coefficient is clearly linearly correlated with the flapper position. This can be noticed by comparing the linear approximation (red line) and table data in the figure. Therefore in fault simulator-type models the linear approximation can be considered to simplify the model.

In the references (Burrows C. R., 1977) and (Wang T., 2005) flow forces in nozzle-flappers are considered, but their construction differs from that used in this study. In these references the construction includes nozzles on both sides of the flapper, as opposed to the one nozzle on one side of the flapper construction used in this study. Therefore the estimated pressure force (flow force) results cannot be compared to the results presented in these references.

The estimation parameters in the mass flow model (6) were the discharge coefficients in Equations $\dot{m}_{in}$ and $\dot{m}_{out}$. For $\dot{m}_{in}$ the estimation parameters were estimated with data captured from the test setup shown in Figure 12 with three different supply pressures, 0,3, 0,5, and 0,7 MPa.

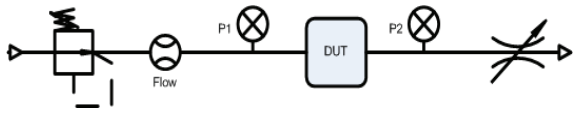

Figure 12. Fixed restrictor test setup (right).

In the measurements the supply pressure was kept constant and the outlet pressure was linearly reduced to the ambient pressure and then increased back to the supply pressure. The device under test (DUT) was just the fixed restrictor, not the complete flapper-nozzle assembly. The results can be seen in Table 3.

Table 3. Fixed restrictor discharge coefficients.

Supply Pressure	0,3MPa	0,5MPa	0,7MPa
Discharge Coefficient	0.92	0.90	0.89

Figure 13 shows one of the estimation data sets used for the discharge coefficient estimation. The discharge coefficient C_d was estimated to be 0.90 when the average was calculated from the results presented in Table 3. The critical pressure ratio $\frac{p_2}{p_1}$ for choked flow was fixed to the ideal value of 0.528. In this case, this agrees well with the measurements, as can be seen from Figure 13.

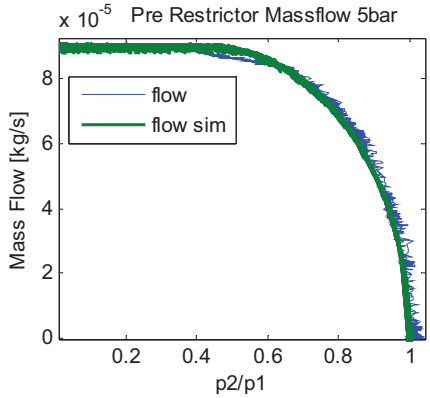

Figure 13. Fixed restrictor mass flow estimation data.

The prestage pressure equation (7) and $\dot{m}_{out}$ in Equation (6) were fitted with the nozzle discharge coefficient lookup table presented in Figure 14. In the measurements the flapper position ramps were run up and down with three different supply pressures, 0,2, 0,5, and 0,8 MPa. The device under test was the entire valve controller. Estimated nozzle discharge coefficient lookup tables are presented in Table 4.

Table 4. Estimated nozzle discharge coefficient lookup tables. 'N/A' means not available as a result of flapper movement range in the conditions being considered.

Flapper Position [mm]	0	0.0350	0.0700	0.1050	Range [mm]
0,2MPa	0.9500	0.9800	0.7800	N/A	0.005-0.075
0,5MPa	0.9500	0.9800	0.8500	0.7000	0.015-0.100
0,8MPa	N/A	0.8800	0.7900	0.7000	0.03-0.105

One of the nozzle discharge coefficient estimation data sets and the average nozzle discharge coefficient lookup table calculated from Table 4 are shown in Figure 14. The flow area in the nozzle is equal to the fixed restrictor in the case where the discharge coefficient starts to decrease noticeably in the discharge coefficient lookup table in the figure. This might indicate that the outlet pressure is not the ambient pressure as a result of restricting elements in the flow path after the nozzle. Other reasons for this kind of discharge coefficient shape might be a poorly modelled nozzle flow area and/or prestage volume.

Discharge coefficient estimation results were not available from other references, but in reference (Wang T., 2005) it was mentioned that the sonic conductance is proportional to the gap between the nozzle and the flapper.

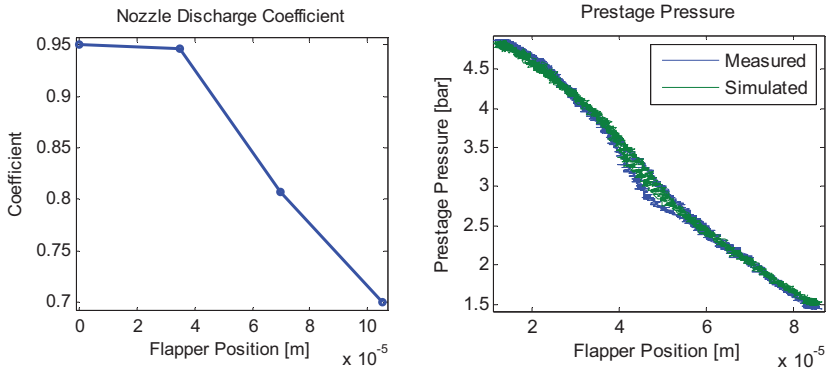

Figure 14. Nozzle discharge coefficient lookup table (left) and prestage pressure (right).

3.2.2 Spool valve

The spool valve model equation (8) was fitted with friction (F_{fs}) and diaphragm forces (F_d). These diaphragm forces were found to be the dominant forces when the static properties of the spool valve were being

considered. Therefore the diaphragm spring forces were measured separately by driving plain unpressurised diaphragms back and forth through a force sensor. The diaphragms were assembled in their nominal position in the spool valve assembly for the measurements. A model for the diaphragms was obtained that was based on the measurements. These measurement data and estimated model outputs are presented in Figure 15.

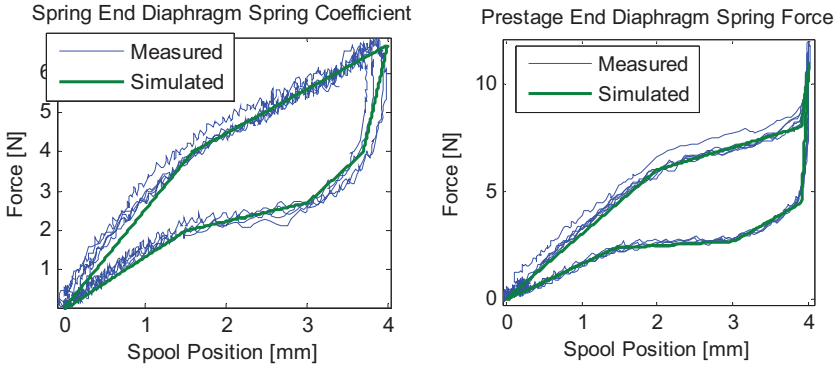

Figure 15. Diaphragm spring forces, spring end (left) and prestage end (right).

The diaphragm models are based on linear spring models defined in specific spool movement ranges. The models take account of both spool valve movement directions to achieve a measured hysteresis in spool valve movement. Because the diaphragm models were estimated without pressure affecting the stiffness of the diaphragms, a separate fitting parameter F_{dCoef} in (10) was needed to apply the effects of pressure to the stiffness of the diaphragm. The estimated diaphragm coefficient is shown in Figure 16. As can be seen from the figure, the pressure and length of the stretching of the diaphragm have an effect on the stiffness of the diaphragms. It should be noted that the diaphragm diameters are different and the supply pressure acts directly on one diaphragm when the prestage pressure is acting on another one.

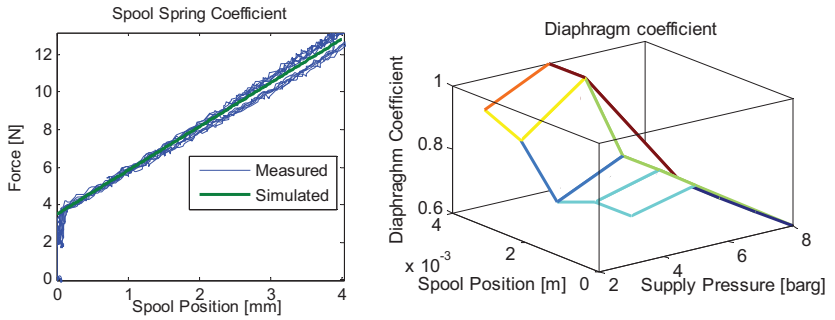

Figure 16. Spool spring coefficient (left) and diaphragm coefficient (right).

The spool spring constant k_{ss} in Equation (9) was also estimated by driving just the spring back and forth through the same force sensor as was used with the diaphragms. The spring was added to the spool valve assembly in its nominal place for measurements. The results of the measurements and simulations can be seen in Figure 16. As can be seen from the figure, the spring acts very linearly and therefore the linear spring model can be applied in the model.

When the static properties of the whole spool valve assembly were tested, elastomer-based hysteresis from the diaphragms completely explains the measured hysteresis in spool movement and can be seen in Figure 17.

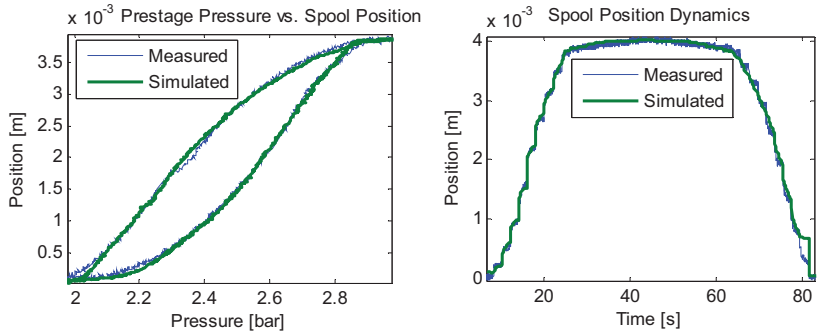

Figure 17. Spool valve static (left) and dynamic (right) estimation data.

The dynamic properties of the spool valve model were estimated with spool valve friction force parameters. One of the estimation data sets is shown in Figure 17. All the friction model parameters were used as estimation parameters. Friction forces were found to be negligible compared to other forces affecting spool movement and therefore are not presented in this study.

The mass flow model (6) through the spool valve was fitted with discharge coefficients, as in the prestage model.

The mass flow filling the actuator cylinder was measured with a mass flow meter with the test setup shown in Figure 12 with three supply pressures, 0,3, 0,5, and 0,8 MPa, and three different spool valve openings, 0.6, 0.8, and 1 (on a scale of 0-1). In the measurements the supply pressure was kept constant and the outlet pressure of the DUT was linearly reduced to the ambient pressure and then increased back to the supply pressure. The DUT in the experiment was the valve controller. Estimated discharge coefficient lookup tables are shown in Table 5, Table 6, and Table 7.

Table 5. Estimated coefficient lookup tables showing the mass flow discharge to the cylinder with 0,3 MPa supply pressure. Rows are for different spool positions [0-1].

P2/p1	0	0.25	0.50	0.75	1
0.6	0.43	0.43	0.42	0.35	0.30
0.8	0.58	0.58	0.57	0.52	0.47
1	0.58	0.58	0.57	0.52	0.47

Table 6. Estimated coefficient lookup tables showing the mass flow discharge to the cylinder with 0,5 MPa supply pressure. Rows are for different spool positions [0-1].

P2/p1	0	0.25	0.50	0.75	1
0.6	0.43	0.43	0.42	0.35	0.30
0.8	0.63	0.63	0.62	0.55	0.50
1	0.63	0.63	0.62	0.55	0.50

Table 7. Estimated coefficient lookup tables showing the mass flow discharge to the cylinder with 0,8 MPa supply pressure. Rows are for different spool positions [0-1].

P2/p1	0	0.25	0.50	0.75	1
0.6	0.43	0.43	0.42	0.35	0.30
0.8	0.63	0.63	0.62	0.55	0.50
1	0.63	0.63	0.62	0.55	0.50

One of the estimation data sets and the estimated fill-in discharge coefficient lookup table are shown in Figure 18. This lookup table is an average lookup table calculated from Table 5, Table 6, and Table 7.

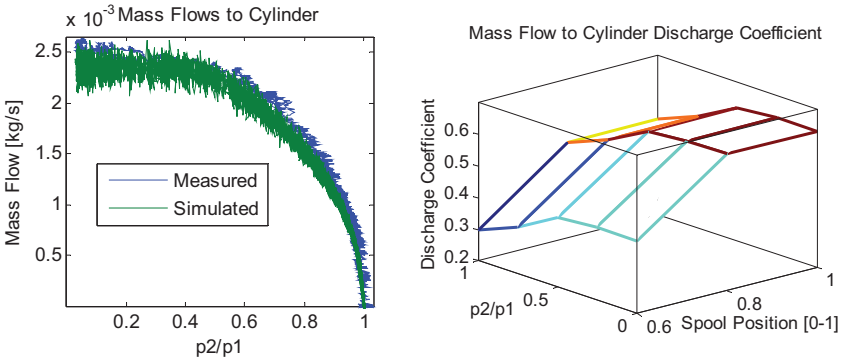

Figure 18. Fill-in mass flow estimation data (left) and flow coefficient (right).

The fixed value of 0.528 for the critical pressure ratio $\frac{p_2}{p_1}$ was again used. This is an acceptable assumption, as shown in Figure 18. It has to be noticed that in this case the estimated discharge coefficient includes several other factors that have an effect, such as secondary pressure losses resulting from the filter regulator, device housing, actuator piping, and connectors. A significant drop in the discharge coefficient within the small spool valve opening might indicate that the spool valve overlap is poorly modelled and therefore the actual flow area is much smaller than that modelled. The lookup table shows that the spool position and the pressure ratio $\frac{p_2}{p_1}$ are equally important factors in defining the discharge coefficient.

In references (Shearer, 1956) and (Richer E., 2000) the fill-in discharge coefficients are estimated to be 0.89 for the spool valves.

The discharge mass flow from the cylinder was measured with a mass flow sensor in the test setup shown in Figure 19.

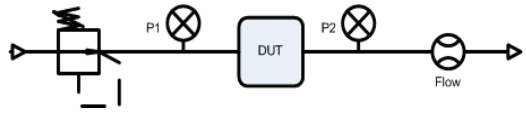

Figure 19. Cylinder discharge mass flow test setup.

In the measurements three spool valve openings, 0, 0.2, and 0.4 (on a scale of 0-1), were used and the differential pressure over the DUT was increased linearly from the ambient pressure to the supply pressure and then reduced linearly back to the ambient pressure. All measurements were performed with three supply pressures, 0,2, 0,5, and 0,8 MPa. The DUT in the experiments was the valve controller. The results of the estimations can be seen in Table 8.

Table 8. Coefficient lookup tables showing the mass flow discharge from the cylinder with 0,2 MPa supply pressure. Rows are for different spool positions [0-1].

Differential Pressure [MPa]	0	0,2	0,5	0,8
0	0.1	0.58	0.60	0.60
0.2	0.1	0.66	0.80	0.80
0.4	0.60	0.70	0.80	0.95

One of the estimation data sets and the estimated discharge coefficient are shown in Figure 20. In the lookup table the cylinder pressure is the determining factor for the discharge flow coefficient, while the effect of the

spool position is minor. The decreasing discharge coefficient related to the increasing spool position might indicate secondary pressure losses, such as the connectors affecting the discharge coefficient in larger spool openings.

In references (Shearer, 1956) and (Richer E., 2000) the discharge coefficients from the cylinder are estimated to be 0.84 for the spool valves.

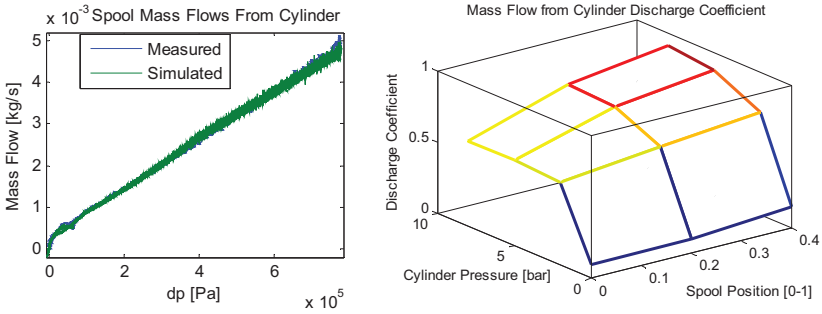

Figure 20. Discharge mass flow (left) and discharge coefficient (right).

3.2.3 Actuator

The actuator model equation (12) was fitted with friction force (11) parameters, especially with the estimated Coulomb friction force parameters shown in Figure 21. These parameters were estimated by driving step series and ramps with an actuator, as shown in Figure 22. Three different supply pressures, 0,35, 0,5, and 0,8 MPa, were used and the estimation results are presented in Table 9 and Table 10.

Table 9. Estimated actuator Coulomb friction forces [N] in positive velocity.

Actuator Position [m]	0	0.0194	0.0388	0.0582	0.0776
0,35MPa	110	100	170	150	130
0,5MPa	110	100	150	130	130
0,8MPa	110	90	130	110	110

Table 10. Estimated actuator Coulomb friction forces [N] in negative velocity.

Actuator Position [m]	0	0.0194	0.0388	0.0582	0.0776
0,35MPa	600	600	550	590	590
0,5MPa	580	580	540	580	580
0,8MPa	580	580	540	580	580

As can be seen from Figure 21, the Coulomb friction force values are notably different. That was the main reason for extending the Karnopp

friction model by adding separate friction parameters for both directions of movement. The Coulomb friction force with positive velocity is correlated with the cylinder pressure, while the negative velocity cylinder pressure can be neglected within the Coulomb friction force.

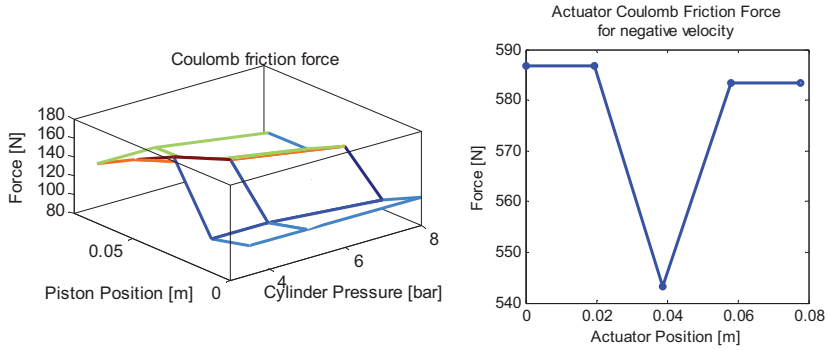

Figure 21. Actuator Coulomb friction forces: for positive velocity (left) and for negative velocity.

It should be noted that the estimated friction forces in this case include several friction forces affecting the system. These are contact friction forces between the piston and cylinder and shaft and sealing, and friction forces acting in joints in the linkage.

In reference (Wang T., 2005) it is also noted that the Coulomb forces are different for positive and negative piston velocities and the cylinder pressure has an influence on the Coulomb friction force.

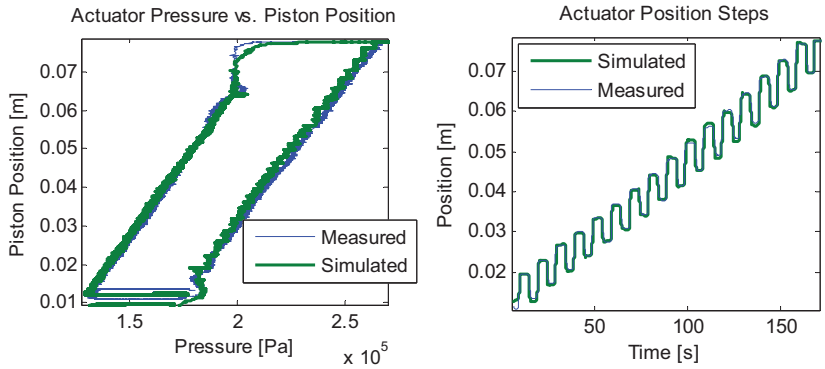

Figure 22. Actuator static and dynamic estimation data.

3.2.4 Process valve

The process valve part of the model was fitted with the friction parameters. The primary estimated parameters were the Coulomb friction coefficients shown in Figure 23. These represent the Coulomb friction coefficients in the

contact between the valve seal and the closing element and are multiplied by the sealing force to obtain the Coulomb friction forces. The sealing force is a load force where the seal is pushing against the closing element. During the estimation test runs the valve seal was loaded through a force sensor to determine the correlation of the seal load with the Coulomb friction force with two different seal loads.

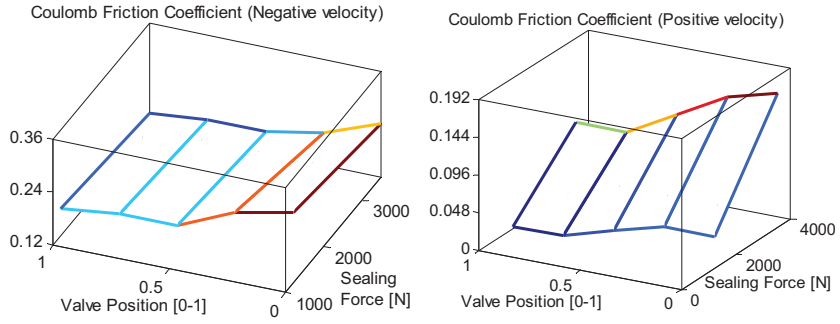

Figure 23. Valve Coulomb friction coefficients.

3.3 Control valve model validation

All the model modules introduced above were connected together to form the complete control valve model. The control valve model was validated first without the valve controller module with step series and ramps. The validation results are seen as control valve's submodule's input-output plots in Figure 24, Figure 25, and Figure 26. They show sufficient agreement between the simulated internal variables and the measured results. That confirms the model is capable of describing all the main nonlinearities and causalities of the system being modelled and that it can be used for fault simulation purposes.

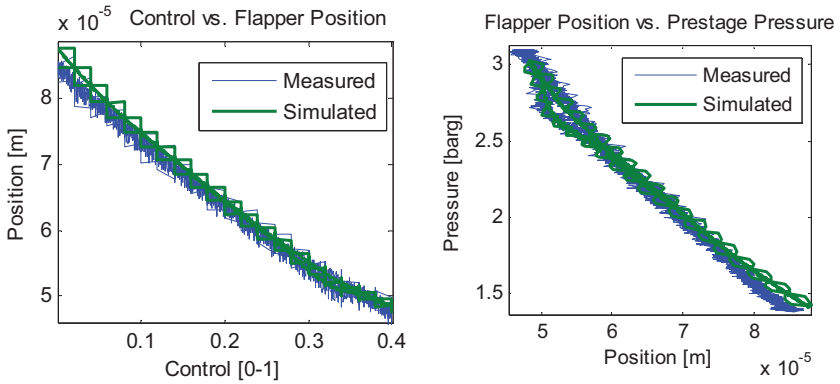

Figure 24. Open loop validation: flapper position (left) and prestage pressure (right)

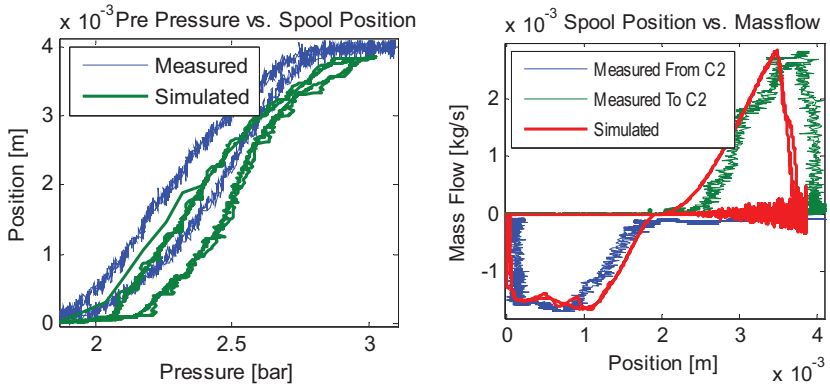

Figure 25. Open loop validation: spool position (left) and spool mass flow (right).

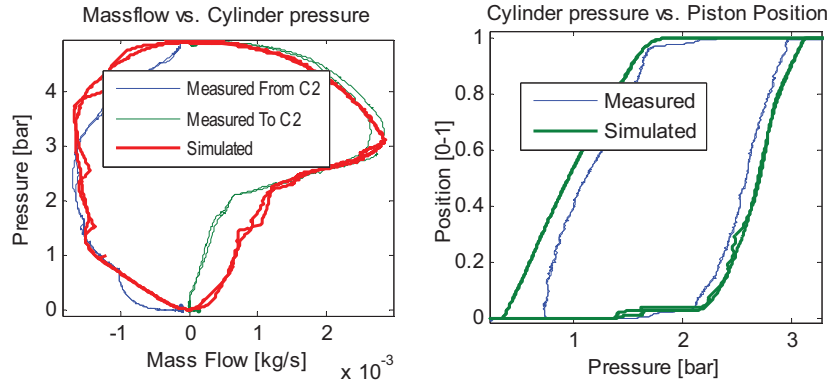

Figure 26. Open loop validation: cylinder pressure (left) and valve position (right).

Then the control valve model was validated with the controller module in place. Some closed loop set point signals and the valve position responses are shown in Figure 27. These figures confirm that the simulator is capable of describing the real behaviour of the control valve and can be used for fault simulation purposes.

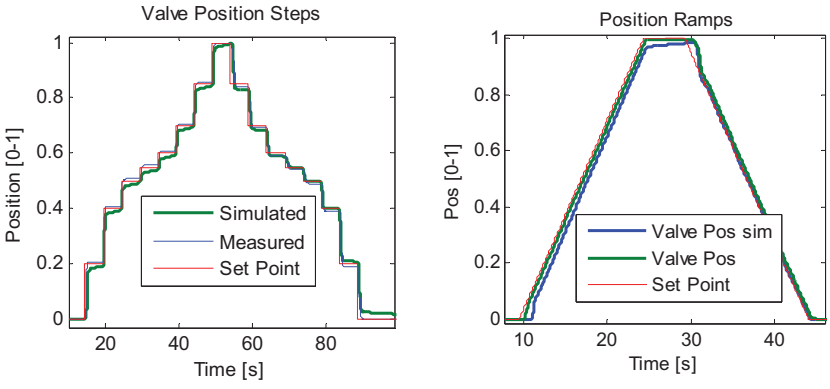

Figure 27. Closed loop set points and responses.

3.4 Fault simulations

Four different fault simulation schemes were run with all faults (presented in Table 1) to research the impact of faults on the system in different valve use cases. These were open loop simulations without any controllers (spool, valve, or flow controller), control valve simulations, and two different flow control loop simulations as presented in Figure 28

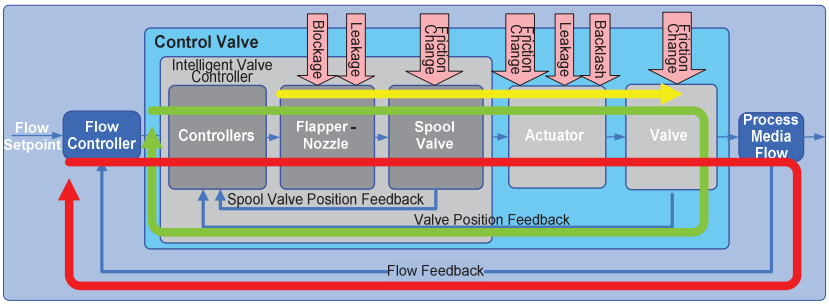

Figure 28. Fault simulations: open loop (yellow), control valve (green), and flow control loop (red).

The simulation results were analysed to research how different faults affect the internal variables and performance of the system. The target was to keep the sizes of the faults small enough to maintain system performance on a good level.

First, open loop simulations were run with ramps and series of steps as a control signal, as shown in Figure 29.

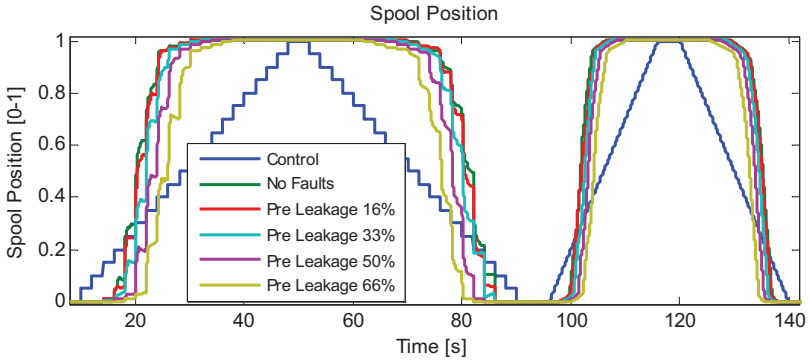

Figure 29. Spool position during open loop simulations (prestage leakage).

Separate simulations were run for different fault magnitudes to simulate the offline performance test use case. The goal of the open loop simulations

was to find out the impacts of faults on a system which did not have controllers compensating for the faults. The variables related to the impacts of the faults that were analysed were all control valve internal variables in the time domain and flow control loop submodule's input-output domain. Examples of these are presented in Figure 30.

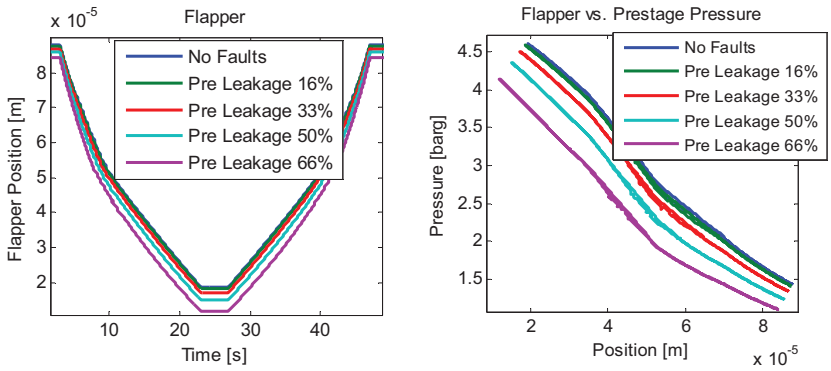

Figure 30. Open loop prestage pressure leakage simulations, flapper position in time domain (left) and module's input-output domain, flapper position vs. prestage pressure (right).

The faults cause operation point changes to the internal variables. With additive faults, such as leakages, this can be seen in the time domain figures and in the module's input-output plots in Figure 30. These figures show how prestage leakage affects the flapper position through the net mass flow to the prestage volume and prestage pressure. The internal variables of the system and variable causalities were presented earlier, in Figure 3.

As a result of the open loop simulations it can be stated that the operation points of the internal variables after the location of a fault in the chain of internal variables are affected by the fault. This is illustrated in Figure 31, where the actuator leakage affects the net mass flow to the actuator and all the operation points of the internal variables after this net mass flow are shifted as a result of the fault. The magnitude of the shift in the operation point shift is related to the size of the fault. The bars in the figure represent the averages of the internal variables during simulations with different quantities of actuator leakage. The averages are scaled to no-fault simulation averages, i.e. zero corresponds to the no-fault situation.

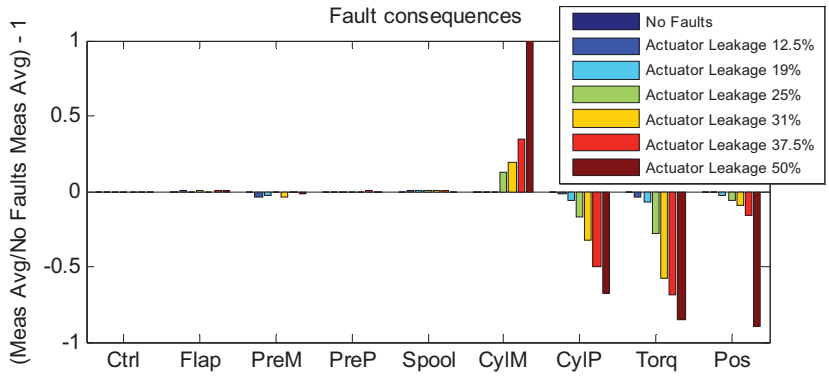

Figure 31. Operation points of the internal variables of the system. The variables in the figure are (from left to right) control signal, flapper position, net mass flow to prestage volume, prestage pressure, spool position, net mass flow to cylinder, cylinder pressure, actuator torque, and valve position.

Second, the control valve simulations were run. These simulated typical offline performance tests performed in process plants and service centres during the servicing of control valves. Therefore separate simulations were run again for different fault magnitudes and ramps and series of steps were used as a control signal, as shown in Figure 32.

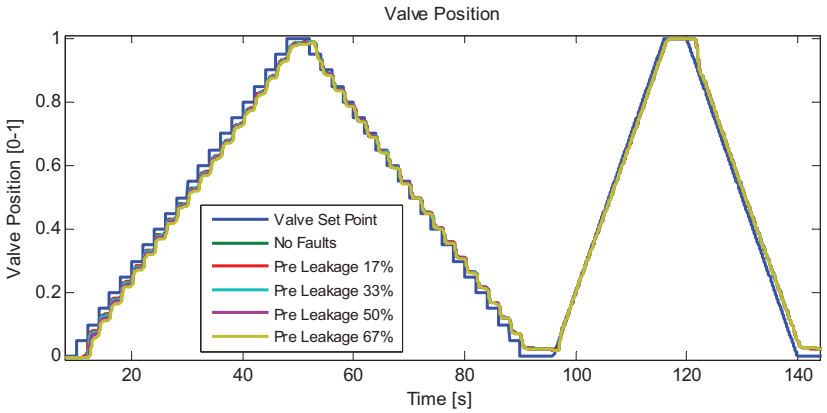

Figure 32. Valve positions during control valve simulations (prestage leakage).

The goal of the control valve simulations was to find out the impacts of faults on a system which has controllers compensating for the faults. The variables related to the impacts of faults that were analysed were again all the control valve internal variables in the time domain and flow control loop submodule's input-output domains. Examples of these are shown in Figure 33. As can be seen in Figure 33, the effects of the faults on the

operation points of the variables were the same as in the open loop simulations.

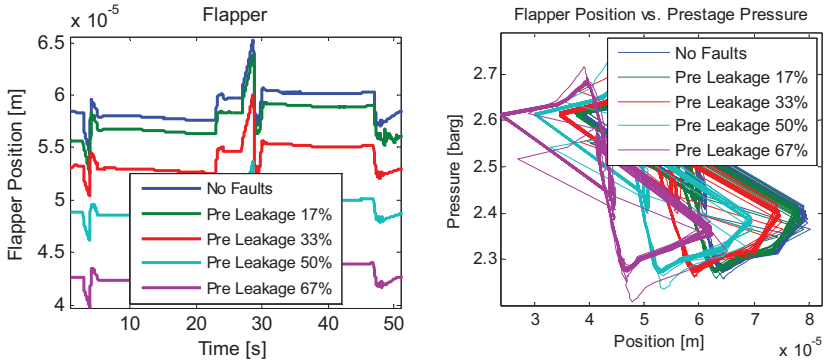

Figure 33. Control valve prestage pressure leakage simulations, flapper position (left), and flapper position vs. prestage pressure (right).

As a result of the control valve simulations it can be noticed that the operation points of the internal variables before the location of a fault in the chain of internal variables are affected by the fault. This is illustrated in Figure 34, where prestage leakage affects the net mass flow to prestage volume and all the operation points of the internal variables before this net mass flow are shifted as a result of the feedback controller trying to compensate for the fault. Compensation for the fault without loss of performance is possible until one of the internal variables saturates.

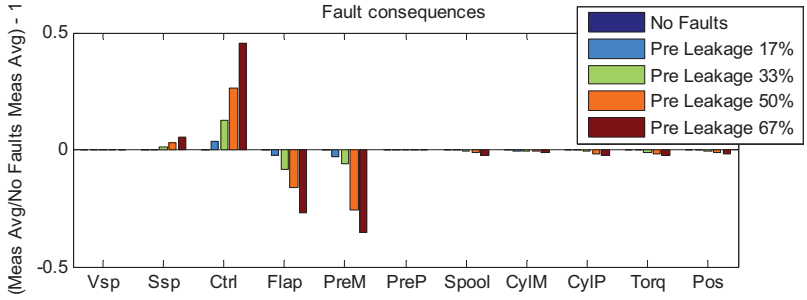

Figure 34. The operation points of the internal variables of the system in flow control loop simulations. The variables in the figure are (from left to right) valve set point, spool set point, control, flapper position, net mass flow to prestage volume, prestage pressure, spool position, net mass flow to cylinder, cylinder pressure, actuator torque, and valve position.

Finally, flow control loop simulations were run. These simulated control valve operation during two separate use cases. These use cases were fast switching and flow control use cases. In the fast switching application the control valve switches between an open and a closed position on a regular

basis, as shown in Figure 35. In the flow control application the control valve can be in a certain position for long periods instead. In the flow control simulations the control valve was only in the same position for short periods so that the simulations could be run through faster.

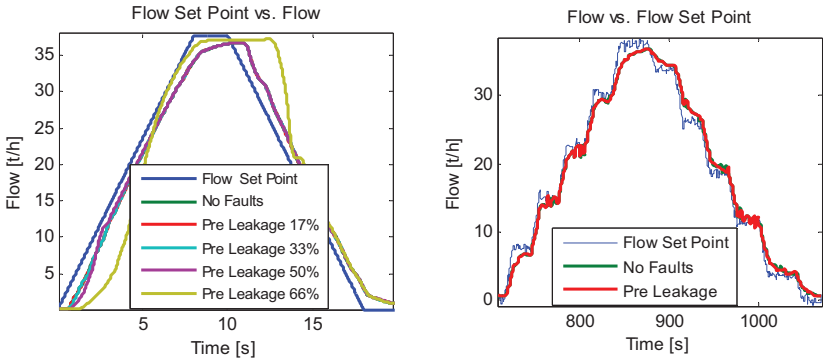

Figure 35. Flow during flow loop simulations, fast switching (left) and flow control (right).

The results from these simulations were consistent with the control valve simulation results presented before. This illustrates that in a feedback control scheme the controllers try to compensate for the fault and this changes in the operation points of the internal variables.

3.5 Discussion

As noted before, it proved possible to analytically model control valve dynamics, despite their inherent nonlinearities. These nonlinearities of the system were estimated through selected fitting parameters. Within this approach the possible nonlinearities of the fixed parameters will also be included in the fitting parameter. This is acceptable, because the motivation for the simulator was to model the system causalities and performance, not to estimate exact parameter values. For this reason, measurement or estimation uncertainty assessments are not performed for the estimated parameters. In other references no comparable results related to the estimated parameters were available and therefore a comparison cannot be performed.

Straightforward models based on an adiabatic process, ideal gas law, and zero upstream velocity were used to keep the model simple and effective. For the same reason, many features were not modelled at all, such as the flow forces acting on the spool valve and leakage flows over the spool valve and cylinder piston.

The only environmental conditions taken into account during the experiments were those related to supply pressure, by using several different supply pressures, while all parameter estimations were made only for data captured at room temperature. The effects of the ambient temperature were only considered within the modelling in some submodels, not within all models. Therefore in future the effects of the ambient temperature on the internal variables have to be researched in more detail.

During the estimations two unexpected findings occurred; the first was the large diaphragm forces in the spool valve assembly, while the second was that there were different Coulomb forces for negative and positive velocity in the pneumatic actuator.

Large diaphragm forces are consequences of robust diaphragm design, but these forces are not a setback for device performance, since the spool valve feedback control loop easily compensates for these kinds of nonlinearities. But consequently diaphragm forces have to be considered in models of this type in the future.

When the Coulomb friction forces are as different as estimated in this study, it is essential to use a proper friction model structure to get sufficient model fitting. In this study the original Karnopp friction model was extended to meet this requirement. The Coulomb friction force was notably greater in the failsafe direction of the actuator. This might indicate that the spring in the actuator pushes the piston in a somehow eccentric manner and the piston does not move so smoothly as in another direction when pressure is pushing the piston.

The models that were derived have been verified with measurements and the modelling error was found to be acceptable for the fault simulations. This means the simulator was capable of representing the causalities and performance of the system being modelled.

Some typical control valve faults have been simulated and their impacts on the internal variables of the flow control loop and control performance analysed. The fault simulator introduced here can be used for fault detection and diagnosis, as well as robust control research. Robust control is an interesting topic in those cases where a fault is diagnosed, but it cannot be fixed before the next planned shutdown, which might be 4 years hence. Then performance should be maintained at an acceptable level within the robust control schematic.

4. Fault detection and diagnosis method for a control valve

As already noted, nowadays valve controllers can detect some symptoms from the control valve without having the capability to pinpoint the real root cause of the fault. This detection is usually based on simple methods such as limit or trend checking. In steady state conditions these methods can be reliable, but when the operation point of the system changes and an alarm limit is set that is related to this specific operation point only, faulty alarms are easily generated. Diagnosing faults correctly and reliably is essential in order to allocate resources effectively to repair the cause of the fault. On the other hand, only information about which module or submodule has to be replaced to repair the problem is required when performing maintenance activities.

Many advanced FDD methods are presented in the literature, as was seen in the *State of the art* section, but implementing these methods in embedded systems is not possible in many cases, because of limited computing power.

At the moment offline tests such as hysteresis and step response tests are used to evaluate control valve performance. This is not an effective method, because the valve has to be isolated from the process for these tests to be run. A more effective method is to perform the diagnosis online during the operation of the device without disturbing the process.

As a conclusion the requirements for a modern FDD method implementable in a valve controller can be listed: system operation point changes should be compensated for, fault localisation should be done at least to sub-modules, diagnosis should be performed online and before the fault has a severe impact on system performance, and finally, the method should require minimal computing power. In the literature review such a method that fulfilled the requirements was not found and therefore it was necessary to develop a new method.

The pneumatic process control valve fault simulator presented earlier makes fault detection and diagnosis research for control valves efficient. In

the fault simulator different fault cases can be simulated, their consequences analysed, data generated for fault detection and diagnosis research, and FDD methods verified.

A new FDD method based on findings related changes in the operation points of the internal variables during fault simulations was developed. In this method the faults can be detected through detecting changes in the operation points of the internal variables. That was observed by analysing the behaviour of the internal variables and submodule's input-output domains of the system during fault simulations. Operation point shifts are the consequences of faults, since feedback control tries to compensate for them. All the internal variables before the location of the fault that has an impact in the chain of internal variables are part of the compensation performed by the controller, as shown in Figure 34. That mechanism enables faults to be localised by detecting the last internal variable affected by the fault. The size of the operation point shift is proportional to the fault size, as also shown in Figure 34. This method was introduced for the first time by the author in the reference (Manninen, 2012).

Figure 34 showed in Chapter 3 how the operation points of the internal variables are shifted by the prestage pressure leakage presented in Figure 36. In the event of this type of fault, the feedback controller compensates for the leakage by moving the flapper closer to the nozzle in the nozzle-flapper system. This reduces the mass flow though the nozzle and maintains the required prestage pressure and spool valve position.

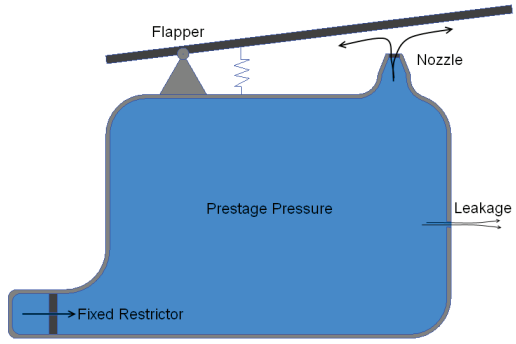

Figure 36. Nozzle-flapper schematics including prestage leakage.

Other system input variables (e.g. set point, supply pressure, temperature) than the faults can also affect the operation points of the internal variables. Therefore the relations between these system input variables and the internal variables have to be modelled in order to separate the effects of

other input variables from the faults. In this case the pneumatic control valve is a highly nonlinear system related to the system input variables. That can be seen from Figure 37, where the effect of the supply pressure and valve set point on the flapper operation point is presented. Therefore nonlinear models should be used for the relations between the input and the internal invariables.

The operation point of the system also has to be taken into account within the diagnostic variables, as shown in Figure 37, where the load factor varies as a function of the valve position, while the actual valve load remains the same all the time. The load factor is a simple diagnostic variable representing the process valve load. If this operation point-related variation is not modelled, the load can triple in small valve openings without a fault being detected, because the high alarm limit is set so high in order to avoid alarms during fault-free operation at all operating points. If the alarm limit is adjusted for one operation point only, faulty alarms are generated when the operation point of the system is changed.

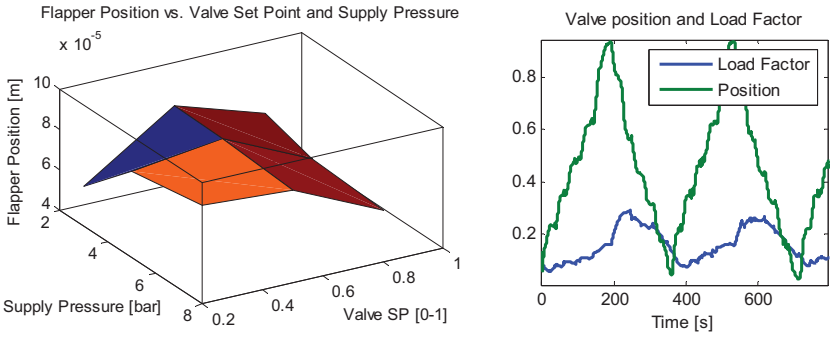

Figure 37. System nonlinearities (left) and the effect of the operation point on the diagnostic variable (right).

In the method introduced here nonlinear relations are modelled through multi-variable histograms.

4.1 Multi-variable histogram models

Multi-variable histogram models are simple statistical nonlinear models of variable relations. The advantages of multi-variable histogram models are their simplicity, ease of learning, and nonlinearity (Friman M., 2007).

As the name of the modelling scheme indicates, Multi-Variable Histogram (MVH) models are based on histograms. As is known, a histogram is a simple way to represent, for example, the distribution of a continuous signal. Basically, an MVH model takes account of the operation point of the

system with the explanatory variables and the model output is the distribution of the variable being observed.

Figure 38 shows an example of a multi-variable model where the relationship between the daily average temperature and observation month is presented. In the model, the month is the explanatory variable for the variable being observed (the temperature) and therefore it indicates the operation point of the system. The output of the model is a temperature histogram in relation to an operation point such as 'in January' (number 1 on the month axis). This temperature distribution also represents the probability distribution of the temperature in the month under consideration. As can be seen from the figure, the most probable average temperature in January is 0 °C and the average temperature typically varies between 5 °C and -20 °C.

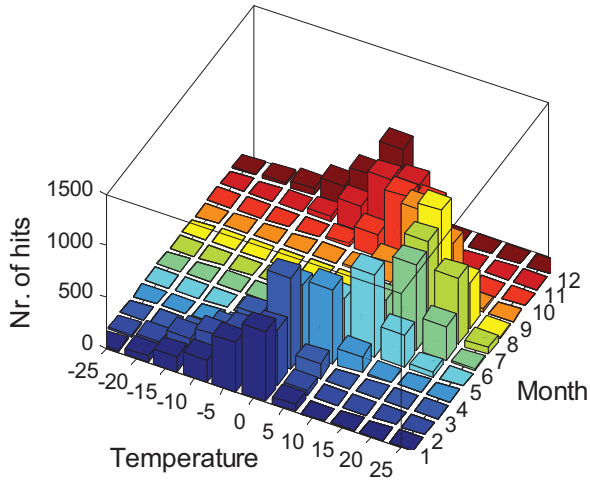

Figure 38. Multi-variable histogram model about outdoor temperature and month. (Friman M., 2007)

When the MVH model includes two explanatory variables, the model is based on schematics where account is taken of the system operation point within the operation point plane, as shown in Figure 39. There the system input variables (Valve Set Point and Supply Pressure) as explanatory variables define the operation point for the variable being observed. As shown in the figure, the operation point plane is divided into 64 bins in this case. One bin represents one operation point of the system and includes a unique histogram as the model output for this operation point.

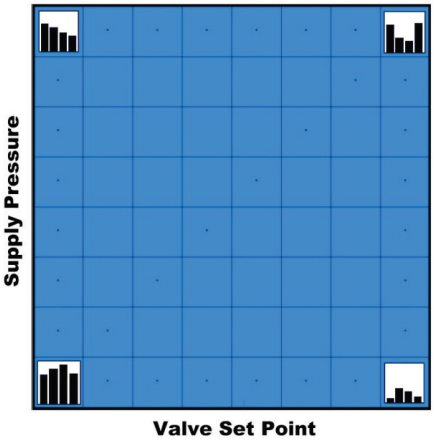

Figure 39. Operation point plane for MVH model including two explanatory variables.

When the effects of other system input variables than faults are taken into account within multivariable histogram model-based schematics, faults can be seen as distribution changes (operation point changes), as presented in Figure 40. In the figure, flapper position distribution is shifted by prestage pressure leakage, as explained earlier.

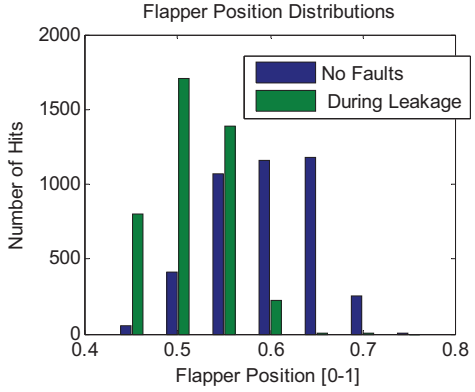

Figure 40. Histogram models at one operation point.

It is essential to research which input variables are the most representative explanatory variables for the variables being observed. It is reasonable to include in the model only those variables which explain the majority of the variation in the variable being observed in order to keep the model structure as simple as possible.

In this study the most representative explanatory variables were searched for by means of information entropy selection functions. Basically, this

means that the input variables producing the largest change in the entropy of the variable being observed were searched for with Equation (16).

$$h = -\sum_i p_i log_2(p_i) \quad (16)$$

Here h is entropy and p_i is the probability, which is estimated from the histogram of the variable by dividing it by the total number of observations. More information about information entropy can be found in, among other references, (Hlavácková-Schindler, 2007).

In this case, the most representative system input variables for each variable being observed are seen in Table 11.

Table 11. Explanatory input variables for variables being observed.

Internal Variable	Explanatory input variables	
Spool SP	Valve SP	
Control	Temperature	Valve SP
Flapper Position	Supply Pressure	Valve SP
Prestage Pressure	Supply Pressure	Valve SP
Spool Position	Valve SP	
Cylinder Pressure	Valve SP	
Valve Load Torque	Valve SP	
Valve Position	Valve SP	
Flow	Valve SP	

Basically, MVH model training puts the observations into the bins defined by the explanatory variables, as in the outdoor temperature example where the January observations were put into the January histogram. Usually forgetting is used to implement adaptation to the normal system variations. The MVH model can also be obtained from the simulation results if the model has to be ready when the device is first operated. When the MVH model is obtained during operation, faults are not allowed to be present in the system to achieve a proper model for FDD applications.

As noted before, the model outputs are distributions. This makes it possible to use a statistical approach for alarm limit generation. In the FDD method introduced here, alarm limits are generated from MVH model distributions. For example, high and low alarm limits can be calculated as limits where 90% of the samples of the distribution are covered around the average of the distribution. Then it can be assumed that the moving average of the variable being observed stays between these limits during fault-free

operation. When these alarm limits are generated for all the histograms located in all the bins in the operation point space, the adaptation of the alarm limit to the system operating point is achieved.

The effect of the operating point on the alarm limits obtained in the way presented above can be seen from Figure 41. In the figure the red lines are alarm limits and the blue line is the moving average of the variable being observed. The figure also shows how prestage leakage affects the flapper position.

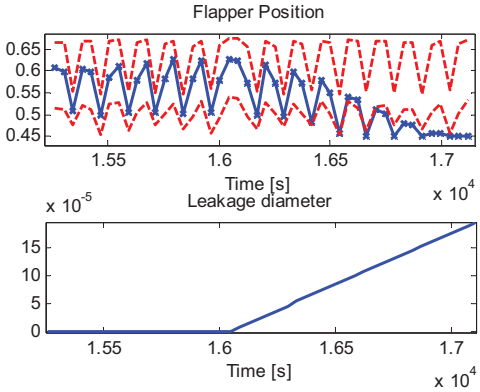

Figure 41. Moving average of flapper position and alarm limits (upper) and prestage leakage path diameter (lower) during prestage leakage simulation.

4.2 FDD method evaluation

The method introduced here was evaluated with fault simulator-generated data, including the 8 different faults shown in Figure 2. Some of the faults were also simulated in a real control valve test bench in the laboratory.

As shown in Figure 42, a noisy stepwise excitation signal was used in the flow control loop simulations during the evaluation. During the simulation environmental variables such as supply pressure and temperature were varied as sinusoidal signals to simulate variations in the real operating environment and therefore verify the robustness of the method that was introduced.

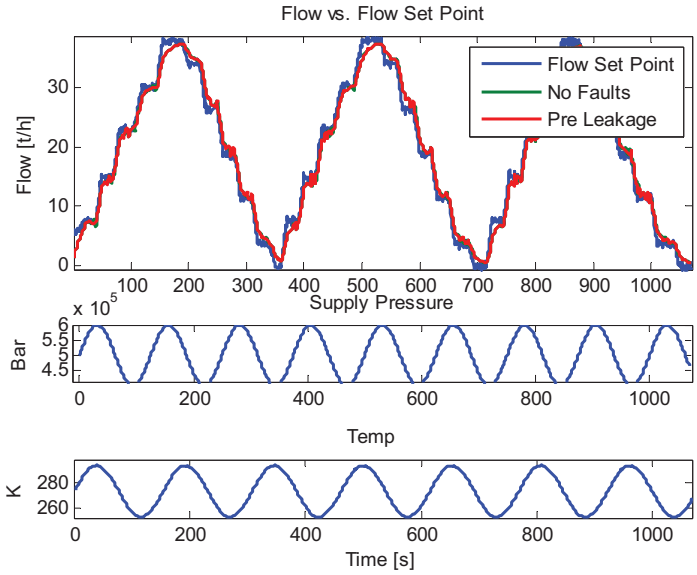

Figure 42. Flow control loop simulation (uppermost), supply pressure (middle) and ambient temperature (lowest).

Every fault (presented in Table 1) that was tested was simulated as a linearly increasing fault. The size of the fault was kept small enough to maintain system performance on a good level. Figure 43 presents the results of prestage leakage simulation as an example. Moving average values of internal variables can be seen in the uppermost figure. Averages are scaled in such a way that the value 0.5 means the variable is close to the average histogram value. As noted before, the flapper compensates for prestage leakage and this can also be seen in the figure when the flapper position deviates strongly from the average position of the histogram. The alarms generated during the simulation by the FDD method introduced here are presented in the middle figure and the size of the fault in the lowest figure.

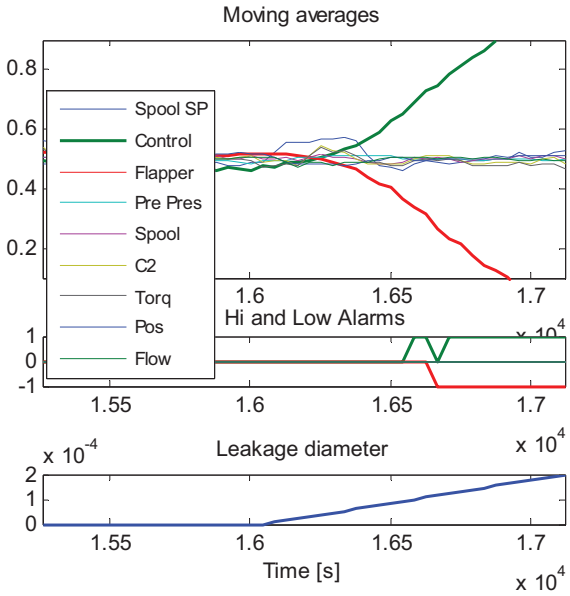

Figure 43. Flow control loop prestage leakage simulation data, internal variable's moving averages (upmost), alarms (middle) and fault size (lowest).

Table 12 shows the results of all the fault simulations run in the fault simulator or in the test bench in the laboratory. The markings in the table are listed below.

- On the left-hand side of the table the internal variables of the system are listed (from top to bottom): spool valve set point, control signal, flapper position, net mass flow to prestage volume, prestage pressure, spool valve position, net mass flow to cylinder, cylinder pressure, valve load torque, and valve position.
- The green area in the table presents the internal variables which should compensate for the fault according to the FDD principle presented before.
- The variables marked in grey were not used in fault detection and diagnosis.
- Simulated faults are listed at the top of the table. The faults behind the numbers are clarified in Table 13.
- The number one stands for the triggered high limit and minus one for the low limit alarm.
- ± means the high and low limit alarms are alternating. This is typical for multiplicative faults, which are related to the sign of the variable being observed.

Table 12. Results of flow control loop fault simulations.

Faults	1	2	3	3.1	4	5	5.1	6	7	8	8.1	9	9.1	10
Spool SP				1		1	1	-1				1	1	
Control	1	-1	1	1	1	1								1
Flapper Pos	-1	1	-1	-1	-1			1						-1
Pre Mass Flow														
Pre Pressure					1			-1						
Spool Pos						1	1	-1				1	1	
C2 Mass flow														
C2 Pressure								±1	±1	-1	-1			-1
Load Torque										±1	±1	±1	±1	±1
Valve Pos														

Table 13 clarifies the fault markings presented in Table 12. The notification 'REAL' in the table means the data were gathered from the real control valve tests run in the laboratory.

Table 13. Fault numbers in Table 12.

	Fault
1	Fixed restrictor blockage
2	Nozzle block
3	Prestage leakage
3.1	Prestage leakage, REAL
4	Spool valve friction
5	Actuator leakage
5.1	Actuator leakage, REAL
6	Actuator friction
7	Actuator backlash
8	Valve friction
8.1	Valve friction, REAL
9	Actuator leakage and Valve friction
9.1	Actuator leakage and Valve friction, REAL
10	Prestage leakage and Valve friction

As can be seen from Table 12, all the faults can be detected and diagnosed to the main modules of the system. Generally, the internal variable closest to the fault reacts to the fault. Therefore the fault can be detected and diagnosed through detecting the internal variables that are affected. The results from the real control valve test bench for three faults that were tested (faults 3.1, 5.1, and 8.1 in Table 12) are consistent with the simulator results. It should also be noticed that some common mode failures (faults 9 and 10 in Table 12) were tested and both faults in these cases were also detected and diagnosed.

4.3 Discussion

On the basis of simulations and test bench test runs, it is possible to detect and diagnose some typical control valve faults before there is a severe impact on flow control loop performance. Anyhow, it should be noticed that some other typical faults, such as sensor faults, are not tested within the method introduced in the simulator. This might not be a problem when it is not necessary to train the method in the faults and it reacts to all possible faults as a result of the principle presented earlier in this study.

Fault detection and diagnosis can be performed with the online method introduced in this study, which requires low computing power. This means the method is implementable in a valve controller and diagnosis can be performed without disturbing the process. The method introduced here has not so far been implemented in an embedded system, but at the moment no obstacles are seen which might prevent that implementation. As shown in Figure 44, one problem with online methods might be the very restricted operating range of the device, meaning that the device can be at the same operation point for months. Therefore it is impossible to detect problems where, for example, the valve load is increased as a result of corrosion in another movement range than that which is now being operated.

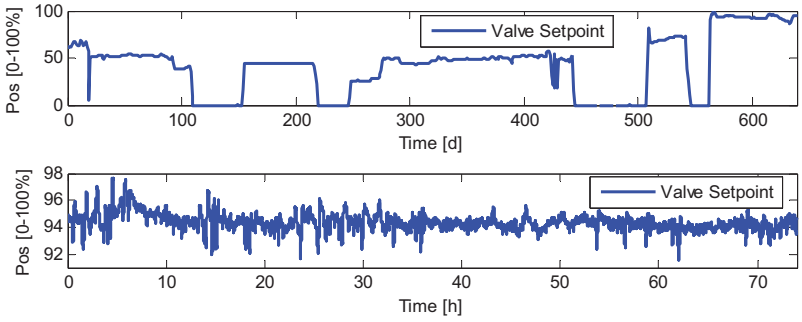

Figure 44. Process control valve set point during a two-year period in the refinery; the upper figure is the daily averages of the valve set points and the lower figure is the valve set points for last three days.

The method introduced here is based on the observation that the internal variable closest to the fault compensates and reacts first to the fault when feedback control is utilised. That leads to an operation point shift for all the internal variables before a fault in the chain of the internal variables in the system. This principle can be utilised in all feedback-controlled mechatronic systems. However, it should be noted that the internal variables and causalities of the system being monitored should be known. Internal mechanical feedbacks should also be recognised from the system in

order to ensure reliable fault detection and diagnosis. When some of the advanced control schematics are utilised, in many cases adaptive models are basic features of the control scheme and therefore a separate model-based FDD model is not needed. But, as stated many times earlier, these advanced methods might be computationally too intensive and therefore not applicable in all embedded systems.

The fault detection and diagnosis method introduced here was verified with simulator and test bench runs and found to be applicable to the detection and diagnosis of all the faults that were tested. This verification was done only with one control valve combination, while the range of products that are supported covers hundreds of different combinations. However, the assumption is that the method introduced here is scalable for different combinations as a result of its universality and adaptation to the system that was monitored. It should also be noted that the method localises the fault naturally rather than diagnosing exactly which fault there is in the system. This is an important aspect when it is impossible to consider all the possible faults which might affect the system being monitored in this kind of very complicated application.

When diagnosis is performed, the prognosis will help to plan maintenance measures. In this case prognosis means a prediction about how a fault or problem will develop in the future. The FDD method developed here might also support this requirement. Because faults affect the operation point of the internal variable and when the physical limits of the internal variable are known, prognosis can be performed by predicting when the internal variable will reach its physical limits and therefore saturate. After saturation system performance will be affected, because the controller cannot compensate for the fault.

5. Conclusions and future research

A fault simulator for a quarter-turn pneumatic control valve is introduced in order to explore the impacts of faults on control valve performance in the flow-controlling loop. The simulator consists of the following models: a valve controller; a pneumatic spring return cylinder actuator; a segment-type process control valve, the flow in the process pipe, and the flow control loop. These analytical models are fitted with some nonlinear fitting parameters, such as position-related spring coefficients. The impacts of some faults on control valve and flow control loop performance are introduced to illustrate the functioning of the simulator. The fault simulator presented here makes possible the research and development of control valve fault diagnosing methods.

In the second part of dissertation a simple fault detection and diagnosis method is introduced. This model-based method is especially suitable for embedded systems because the need for computing power is minimal. In this method, the static model scheme is utilised to model inherent system nonlinearities. When the explanatory variables are specified, the model is obtained during system operation. Knowledge of the model structure or fault learning is not needed. The method introduced here is applicable for all systems where feedback control is utilised and some of the system's internal variables are measurable.

In this method the faults can be detected through detecting changes in the operation points of the internal variables. These operation point changes are consequences of the faults, since feedback control tries to compensate for them. All the internal variables in the chain of internal variables before the impact of the location of the fault are part of the compensation performed by the controller. That mechanism enables faults to be localised by detecting the last internal variable affected by the fault. The size of the change in the operation point is proportional to the fault size. Other system input variables (e.g. set point, supply pressure, temperature) than the faults can also affect the operation points of the internal variables. Therefore the relations of these input variables to the internal variables have to be modelled to differentiate the effects of other input variables from the faults.

In this case these relations are modelled by multi-variable histograms. Multi-variable histograms are simple statistical nonlinear models of variable relations.

Eight typical faults, such as leakages, friction changes, and backlash for the process control valve, were simulated in the process control valve fault simulator and the proposed method was tested. The results show that all faults (presented in Table 1) can be detected and diagnosed before there is a severe impact on the control performance of the system. Some of the faults were also tested on a real process control valve in the laboratory. The results in the real environment are consistent with the simulator results.

The next research steps might be:

- the effects of ambient temperature on the internal variables, because the ambient temperature might be the explanatory variable for many internal variables;
- optimisation of the quantity of the operation point space bins and the histogram sections;
- optimisation of the observed variables needed to localise the faults to the required accuracy;
- verification of the method with other control valve combinations, because there are numerous different actuator and valve types and sizes in the range of products that are supported;
- the sensor faults and how these are detected within the method introduced here;
- Can prognosis done after the fault has been detected and diagnosed;
- robust control after the fault has been detected and diagnosed.

6. References

Balle P., Fuessel D., Closed-loop fault diagnosis based on a nonlinear process model and automatic fuzzy rule generation, Engineering Applications of Artificial Intelligence, 2000, Vol. 13, pp. 695-704.

Baranyi P., Korondi P., Patton R. J., Hashimoto H., Trade-off between approximation accuracy and complexity for ts fuzzy models, Asian Journal of Control, 2004, Vol. 6, pp. 21-33.

Bartys M., Patton R., Syfert M., de las Heras S., Quevedo J., Introduction to the DAMADICS actuator FDI benchmark study, Control Engineering Practice, 2006, Vol. 14, pp. 577-596.

Bartys M. Z., Koscielny J. M., Application of fuzzy logic fault isolation methods for actuator diagnosis, IFAC 15th Triennial World Congress, Barcelona, 2002.

Bocănială C. D., Sa da Costa J., Application of novel fuzzy classifier to fault detection and isolation of the DAMADICS benchmark problem, Control Engineering Practice, 2006, Vol. 14, pp. 653–669.

Burrows C. R., Peckham R. G., Dynamic characteristics of a pneumatic flapper valve, Journal Mechanical Engineering Science, 1977, Vol. 19, pp. 113-121.

Calado J.M.F., Sa da Costa J.M.G., Bartysc M., Korbicz J., FDI approach to the DAMADICS benchmark problem based on qualitative reasoning coupled with fuzzy neural networks, Control Engineering Practice, 2006, Vol. 14, pp. 685–698.

Choudhury M. A. A. S., Detection and diagnosis of control loop nonlinearities, valve stiction and data compression, University of Alberta, 2005, Dissertation.

Choudhury M.A.A. S., Thornhill N.F., Shah S.L., Modelling valve stiction, Control Engineering Practice, 2005, Vol. 13, pp. 641–658.

Deibert R., Model based fault detection of valves in flow control loops, Safeprocess 1994, Helsinki, 1994, pp. 445-450.

Driskell L., Control Valve Selection and Sizing, Instrument Society of America (ISA), 1983.

Friman M., Happonen H., Managing adaptive process monitoring: new tools and case examples, Proceedings of the IEEE Mediterranean Conference on Control and Automation, 2007, pp. 27–29.

Garcia C., Comparison of friction models applied to a control valve, Control Engineering Practice, 2008, Vol. 16, pp. 1231–1243.

Garcia C., Friction model parameter estimation for control valves, 8th International IFAC Symposium on Dynamics and Control of Process Systems, Cancún, 2007. pp. 273-278.

Heras S. de las, Improving gas dynamic models for pneumatic systems, International Journal of Fluid Power, 2003, Vol. 4, pp. 47-56.

Hlavácková-Schindler K., Paluš, M., Vejmelka, M., Bhattacharya, J., Causality detection based on information-theoretic approaches in time series analysis, Physics Reports, 2007, Vol. 441, pp. 1-46.

Kagawa T., Heat transfer effects on the frequency response of a pneumatic nozzle flapper, Journal of Dynamic Systems, Measurement, and Control, 1985, Vol. 107, pp. 332-336.

Kano M., Maruta H., Kugemoto H., Shimizu K., Practical model and detection algorithm for valve stiction, IFAC, 2004

Karnopp D., Computer simulation of stick-slip friction in mechanical dynamic systems, ASME J. of Dynamic Systems, Measurement and Control, 1985, Vol. 107, pp. 100-103.

Karpenko M., Sepehri N., Scuse D., Diagnosis of process valve actuator faults using a multilayer neural network, Control Engineering Practice, 2003, Vol. 11, pp. 1289–1299.

Kayihan A., Doyle F. J., Friction compensation for a process control valve, Control Engineering Practice, 2000, Vol. 8, pp. 799-812.

Korbicz J., Kowal M., Neuro-fuzzy networks and their application to fault detection of dynamical systems, Engineering Applications of Artificial Intelligence, 2007, Vol. 20, pp. 609–617.

Ling B., Zeifman M., Liu M., A Practical System for Online Diagnosis of Control Valve Faults, Proceedings of the 46th IEEE Conference on Decision and Control, New Orleans, 2007, pp. 2572-2577.

Manninen T., Fault Detection and Diagnosis Method for a Process Control Valve, 8th International Fluid Power Conference, Dresden, Technische Universität Dresden, 2012, Vol. 3, pp. 499-508.

Manninen T., Schlupp K., Process control valve fault simulator, The Twelfth Scandinavian International Conference on Fluid Power, SICFP'11., Tampere, Tampere University of Technology, 2011., Vol. 4. pp. 41-56.

Mare J.-C., Geider O., Colin S., An improved dynamic model of pneumatic actuators, International Journal of Fluid Power, 2000, Vol. 1, pp. 39-47.

McGhee J., Henderson I. A., Baird A., Neural networks applied for the identification and fault diagnosis of process valves and actuators, Measurement, 1997, Vol. 20. pp. 267-275.

Mendonca L.F., Sousa J.M.C., Sa da Costa J.M.G. An architecture for fault detection and isolation based on fuzzy methods, Expert Systems with Applications, 2009, Vol. 36, pp. 1092–1104.

Mina J., Verde C., Fault detection using dynamic principal component analysis by average estimation, 2nd International Conference on Electrical and Electronics Engineering (ICEEE) and XI Conference on Electrical Engineering (CIE 2005), Mexico City, 2005, pp. 374-377.

Mrugalski M., Witczak M., Korbicz J., Confidence estimation of the multi-layer perceptron and its application in fault detection systems, Engineering Applications of Artificial Intelligence, 2008, Vol. 21, pp. 895–906.

Patton F. J., Uppal R. J., Neuro-fuzzy uncertainty de-coupling: a multiple-model paradigm for fault detection and isolation, International Journal of Adaptive Control and Signal Processing, 2005, Vol. 19, pp. 281–304.

Puig V., Witczak M., Nejjari F., Quevedo J., Korbicz J., A GMHD neural network-based approach to passive robust fault detection using a constraint satisfaction backward test, Engineering Applications of Artificial Intelligence, 2007, Vol. 20, pp. 886–897.

Pyötsiä J., A Mathematical Model of a Control Valve, Helsinki University of Technology, 1991, Dissertation.

Raparelli T., Bertetto A. M., Mazza L., Experimental and numerical study of friction in an elastomeric seal for pneumatic cylinders, Tribology International, 1997, Vol. 30, pp. 547-552.

Ravanbod-Shirazi L., Besancon-Voda A., Friction identification using the Karnopp model, applied to an electropneumatic actuator, J. Systems and Control Engineering, 2003, Vol. 217, pp. 123-.

Richer E., Hurmuzlu Y., A high performance pneumatic force actuator system: part I - nonlinear mathematical model, Journal of Dynamic Systems, Measurement, and Control, 2000, Vol. 122, pp. 416-425.

Romano R. A., Garcia C., Comparison between two friction model parameter estimation methods applied to control valves, 8th International IFAC Symposium on Dynamics and Control of Process Systems, Cancún, 2007, Vol. 2, pp. 202-208.

Schroeder L. E., Singh R., Experimental study of friction in a pneumatic actuator at constant velocity, Journal of Dynamic Systems, Measurement, and Control, 1993, Vol. 115, pp. 575-577.

Sharif M. A., Grosvenor R. I. Fault diagnosis in industrial control valves and actuators, IEEE Instrumentation and Measurement Technology Conference, St. Paul, 1998, pp. 770-778.

Sharif M. A., Grosvenor R. I., Sensor-based performance monitoring of a control valve unit, Journal of Process Mechanical Engineering, 1999, Part E, Vol. 213, pp. 71-84.

Sharif M. A., Grosvenor R. I., The development of novel control valve diagnostic software based on the visual basic programming language, Journal of Process Mechanical Engineering, 2000, Part I, Vol. 214, pp. 99-125.

Shearer J. L., Nonlinear analog study of a high-pressure pneumatic servomechanism, Transactions of the ASME, 1957, pp. 465-472.

Shearer J. L., Study of pneumatic processes in the continuous control of motion with compressed air – I, Transactions of the ASME, 1956, pp. 233-242.

Shearer J. L., Study of pneumatic processes in the continuous control of motion with compressed air – II, Transactions of the ASME, 1956, pp. 243-249.

Sorli M., Gastaldi L., Thermic influence on the dynamics of pneumatic servosystem, Journal of Dynamic Systems, Measurement, and Control, 2009, Vol. 131

Srinivasan R., Rengaswamy R., Nallasivam U., Rajavelu V., Issues in modeling stiction in process control valves, 2008 American Control Conference, Seattle, 2008, pp. 3374-3379.

Uppal F. J., Patton R. J., Fault diagnosis of an electro-pneumatic valve actuator using neural networks with fuzzy capabilities, ESANN'2002 proceedings - European Symposium on Artificial Neural Networks, Bruges, 2002, pp. 501-506.

Uppal F. J., Patton R. J., Witczak M., A neuro-fuzzy multiple-model observer approach to robust fault diagnosis based on the DAMADICS benchmark problem, Control Engineering Practice, 2006, Vol. 14, pp. 699–717.

Wang T., Cai M., Kawashima K., Kagawa T., Modelling of nozzle - flapper type pneumatic servo valve including the influence of flow force, International Journal of Fluid Power, 2005, Vol. 6, pp. 33-43.

Várkonyi-Kóczy A. R., Baranyi P., Patton R. J., Anytime fuzzy modeling approach for fault detection systems, IMTC 2003 – Instrumentation and Measurement Technology Conference, Vail, 2003

Virvalo T., Modeling and Design of a Pneumatic Position Servo System Realized with Commercial Components, Tampere, Tampere University of Technology, Publications 171, 1995, p. 197, Dissertation.

Zhi Xiang, Ivan L., Lakshminarayanan S., A New Unified Approach to Valve Stiction Quantification and Compensation, Ind. Eng. Chem. Res, 2009, Vol. 48, pp. 3474–3483.

In this study a novel fault simulator for a quarter-turn pneumatic process control valve is presented. It is based on analytical models and all nonlinearities of the system have been identified and estimated through selected parameters. Some typical control valve faults have been simulated and the impacts on the internal variables of the flow control loop and control performance analysed. The fault simulator presented here can be used for fault detection and diagnosis, as well as robust control research. On the basis of simulations and test bench test runs it is possible to detect and diagnose typical control valve faults before they have a severe impact on flow control loop performance. This can be done with the online method introduced in this study, which requires low computing power.

Aalto-DD 146/2012

ISBN 978-952-60-4853-6
ISBN 978-952-60-4854-3 (pdf)
ISSN-L 1799-4934
ISSN 1799-4934
ISSN 1799-4942 (pdf)

Aalto University
School of Engineering
Department of Engineering Design and Production
www.aalto.fi

BUSINESS + ECONOMY

ART + DESIGN + ARCHITECTURE

SCIENCE + TECHNOLOGY

CROSSOVER

DOCTORAL DISSERTATIONS